

8901 977

1

PL-TR-94-2076

AD-A280 948



**CONTINUED STUDIES OF POLAR CAP
THERMOSPHERIC DYNAMICS**

**T. L. Killeen
R. J. Niecejewski**

**DTIC
ELECTE
JUN 07 1994
S F D**

**University of Michigan
Space Physics Research Laboratory
Dept of Atmospheric, Oceanic & Space Sciences
Ann Arbor, MI 48109**

March 1994

DTIC QUALITY INSPECTED 8

**Final Report
23 October 1989-23 January 1993**

Approved for public release; distribution unlimited

94-16999



**PHILLIPS LABORATORY
Directorate of Geophysics
AIR FORCE MATERIEL COMMAND
HANSCOM AIR FORCE BASE, MA 01731-3010**

94 6 6 051

"This technical report has been reviewed and is approved for publication"


EDWARD J. WEBER
Contract Manager


EDWARD J. BERGHORN
Branch Chief


WILLIAM K. VICKERY
Division Director

This document has been reviewed by the ESD Public Affairs Office (PA) and is releasable to the National Technical Information Service (NTIS).

Qualified requestors may obtain additional copies from the Defense Technical Information Center. All others should apply to the National Technical Information Service.

If your address has changed, or if you wish to be removed from the mailing list, or if the addressee is no longer employed by your organization, please notify PL/TSI, Hanscom AFB, MA 01731-5000. This will assist us in maintaining a current mailing list.

Do not return copies of this report unless contractual obligations or notices on a specific document requires that it be returned.

REPORT DOCUMENTATION PAGE

Form Approved
OMB No. 0704-0188

Public reporting burden for this collection of information is estimated to average 1 hour per response, including the time for reviewing instructions, searching existing data sources, gathering and maintaining the data needed, and completing and reviewing the collection of information. Send comments regarding this burden estimate or any other aspect of this collection of information, including suggestions for reducing this burden, to Washington Headquarters Services, Directorate for Information Operations and Reports, 1215 Jefferson Davis Highway, Suite 1204, Arlington, VA 22202-4302, and to the Office of Management and Budget, Paperwork Reduction Project (0704-0188), Washington, DC 20503.

1. AGENCY USE ONLY (Leave blank)		2. REPORT DATE March 1994	3. REPORT TYPE AND DATES COVERED Final (23 Oct 1989-23 Jan 1993)	
4. TITLE AND SUBTITLE Continued Studies of Polar Cap Thermospheric Dynamics			5. FUNDING NUMBERS PE 61102F PR 2310 TA G9 WU AK	
6. AUTHOR(S) T. L. Killeen R. J. Niciejewski			Contract F19628-89-K-0047	
7. PERFORMING ORGANIZATION NAME(S) AND ADDRESS(ES) The University of Michigan Space Physics Research Laboratory Dept of Atmospheric, Oceanic and space Sciences Ann Arbor, MI 48109			8. PERFORMING ORGANIZATION REPORT NUMBER	
9. SPONSORING / MONITORING AGENCY NAME(S) AND ADDRESS(ES) Phillips Laboratory 29 Randolph Road Hanscom AFB, MA 01731-3010 Contract Manager: Edward Weber/GPIA			10. SPONSORING / MONITORING AGENCY REPORT NUMBER PL-TR-94-2076	
11. SUPPLEMENTARY NOTES				
12a. DISTRIBUTION / AVAILABILITY STATEMENT Approved for public release; distribution unlimited			12b. DISTRIBUTION CODE	
13. ABSTRACT (Maximum 200 words) The primary scientific goal for the Thule Greenland optical facility was to acquire measurements of upper thermospheric winds and temperatures during the dark optical observing season. The data acquired by the Fabry-Perot interferometer has been used to extend the thermospheric database coverage for Thule from the initial December 1985 period to the conclusion of the 1990/91 observing season. The initial observations have been used in concert with the NCAR Thermospheric General Circulation Model to improve the understanding of the thermodynamics of the polar cap ionosphere. The airglow facility at Thule AB is the high-latitude anchor of a latitudinal chain of Fabre Perot interferometer stations devoted to observing the OI (6300A) emission feature. Thus, the F region measurements obtained at Thule AB provide valuable data in a global effort at improving our understanding of the dynamic state of the upper atmosphere.				
14. SUBJECT TERMS Thermosphere winds Fabry-Perot interferometer			Neutral winds	
			15. NUMBER OF PAGES 56	
			16. PRICE CODE	
17. SECURITY CLASSIFICATION OF REPORT Unclassified	18. SECURITY CLASSIFICATION OF THIS PAGE Unclassified	19. SECURITY CLASSIFICATION OF ABSTRACT Unclassified	20. LIMITATION OF ABSTRACT SAR	

TABLE OF CONTENTS

Introduction	1
Experimental Aspects of the Thule Facility	2
Results	4
Summary	5
References	7
Figure Captions	8

Appendix A:

Journal Articles

Killeen, T. L., F. G. McCormac, A. G. Burns, J. P. Thayer, R. M. Johnson, and R. J. Niciejewski, On the dynamics and composition of the high-latitude thermosphere, *J. Atmos. Terr. Phys.*, 53, 797, 1991.

Niciejewski, R. J., T. L. Killeen, R. M. Johnson, and J. P. Thayer, The behavior of the high-latitude F-region neutral thermosphere in relation to IMF parameters, *Adv. Space Res.*, 12, (6)215, 1992.

Appendix B:

Presented at conferences

F-region neutral winds at Søndre Strømfjord: IMF B_y and B_z dependences from Fabry-Perot and incoherent scatter measurements

An investigation of a polar cap arc sequence using ground-based measurements at Thule, Greenland

Ground-based OI (6300Å) Fabry Perot interferometer observations from Thule and Søndre Strømfjord, Greenland: systematics in the F region neutral winds observed concurrently by both instruments

Ground-based observations of ion/neutral coupling at Thule and Qanâq, Greenland: IMF B_z dependence

The behaviour of the high-latitude F-region neutral thermosphere in relation to IMF parameters

Fabry Perot interferometer observations of neutral winds in the polar cap during northward IMF

Ground-based optical measurements from within the geomagnetic polar cap at Thule, Greenland ($\Lambda=86^\circ$)

Observations of neutral winds in the polar cap during northward IMF

Seasonal and diurnal variability in the northern high latitude thermosphere: neutral temperatures and horizontal winds

The northern, high latitude thermosphere: neutral temperatures and winds during the 1991/92 optical observing season

Observations of high-latitude thermospheric neutral winds over a half solar cycle from Thule Air Base and Søndre Strømfjord, Greenland

Fabry-Perot interferometric measurements of mesopause and lower thermospheric structure

Studies of high-latitude lower thermospheric dynamics based on measurements and modelling of lower thermospheric coupling study experiments

Seasonal variation of winds in the high latitude lower thermosphere/upper mesosphere at Thule Air Base and Søndre Strømfjord, Greenland

Tides in the lower thermosphere and upper mesosphere from optical and radar measurements and model results

Thermospheric neutral wind climatology in the northern high latitudes

Appendix C:

PhD Theses

Thayer, J. P., Neutral wind vortices in the high-latitude thermosphere, 1990

Won, Y., Studies of thermospheric neutral winds utilizing ground-based optical and radar measurements, 1994

Accession For	
NTIS CRA&I	<input checked="" type="checkbox"/>
DTIC TAB	<input type="checkbox"/>
Unannounced	<input type="checkbox"/>
Justification	
By	
Distribution /	
Availability Codes	
Dist	Avail and/or Special
A-1	

INTRODUCTION

The primary scientific goal for the Thule optical facility was to acquire measurements of upper thermospheric winds and temperatures during the dark observing seasons covered by this report: the months September to April and the seasons 1989/90 and 1990/1. Unfortunately, funding for the original three year effort was terminated at the end of the second year: October, 1991. Secondary goals were 1) to continue a lower thermospheric wind and temperature measurement program with the Fabry Perot interferometer established in the previous report period; 2) to continue the measurement program of the AFGL spectrophotometer; 3) to field an all sky camera system; 4) to test a near infrared Michelson interferometer; and 5) to support various NSF, AFGL, and CEDAR sponsored measurement campaigns.

The data acquired by the Fabry Perot interferometer has been used to extend the thermospheric database coverage for Thule from the initial December, 1985, period to the conclusion of the 1990/1 observing season. The initial observations have been used in concert with the NCAR Thermospheric General Circulation Model to improve the understanding of the thermodynamics of the polar cap ionosphere [Killeen *et al.*, 1991; Niciejewski *et al.*, 1992; Niciejewski and Killeen, 1992; Niciejewski *et al.*, 1993; Thayer *et al.*, 1994; Johnson *et al.*, 1994; Niciejewski *et al.*, 1994]. The airglow facility at Thule Air Base is the high latitude anchor of a latitudinal chain of Fabry Perot interferometer stations devoted to observing the OI (6300 Å) emission feature. Thus, the F region measurements obtained at Thule Air Base provide valuable data in a global effort at improving our understanding of the dynamic state of the upper atmosphere.

The Ebert Fastie spectrophotometer has been used to observe emissions from various nightglow features including NI (5200 Å), OI (5577 Å), OI (6300 Å), Balmer H α (6563 Å), OII (7320/30 Å), and the OH (8-3) vibrational band. In addition, several of these features are enhanced in aurora, and thus the spectrophotometer serves as an auroral monitor aiding the interpretation of lower thermospheric temperature measurements. Interpretation of the rotational development of the hydroxyl band permits the investigation of temperature, gravity wave, and tidal motions at the mesopause. In addition, lower atmosphere scattering from air base Hg vapor lamps was monitored and served as an indicator of sky transparency conditions.

The second trailer was modified by adding an internal wall to make two separate rooms, and by adding a second dome. An all sky camera was housed under a dome in the new trailer during the 1988/9 observing season. The sky was observed through several filters including OI (5577 Å), OI (6300 Å), and OII (7320/30 Å) for the purpose of coordinating measurements of sun aligned arcs with both the Fabry Perot interferometer and the Ebert Fastie spectrophotometer. A Michelson interferometer was placed under the second dome and operated for one winter season observing mesospheric hydroxyl airglow emissions. The current layout of the Thule facility is shown in Figure 1. The original trailer with its two domes is in the foreground and the new trailer is on the right.

The optical facility has been in operation during most of the winter CEDAR campaigns during the report period. Data has been acquired for several LTCS and HLPS campaigns as well as for GITCAD/GISMOS and other global efforts.

This final report will summarize optical facility activity in Thule, present results from the various experiments, and describe work that is currently in progress. Included are reprints of papers published in geophysical journals, and several abstracts of papers pre-

sented or to be presented at AGU meetings. Two graduate student theses are based on data acquired at Thule Air Base and a report on the conclusion of their research is included.

EXPERIMENTAL ASPECTS OF THE THULE AIR BASE FACILITY

Up to four instruments have operated under separate domes at the Thule Air Base airglow facility in Greenland. The primary instrument is the Fabry Perot interferometer, and this is supplemented by an Ebert Fastie spectrophotometer, an all sky camera system, and a Michelson interferometer. The Fabry Perot interferometer has been observing the OI (6300 Å) emission line profile since the start of operation of the Thule ground site. The scan sequence includes a measurement in the zenith followed by observations in the four cardinal directions at elevation angles of 45 degrees. The typical integration period is a few minutes for a 100 Rayleigh signal and is determined primarily by waiting for the signal minus background count to exceed a predetermined minimum. The statistical uncertainties for neutral winds and temperatures are on the order of 15 m/sec and 50 K respectively. In addition to monitoring the sky signal, a Ne lamp emission at 6330 Å is also observed. This is accomplished by moving the mirror system to a position that looks into the box containing the calibration source. By calculating a pseudo wind from the Ne emission, any drifts in the stability of the instrument may be taken into account. Typically, in any 24 hour period, the instrument remains stable to within 25 m/sec. Finally, the dark count rate is also monitored and removed from the sky signal.

The most important new contribution from the operation of the Fabry Perot interferometer was the monitoring of the lower thermosphere. This was accomplished as a response to the desire from the CEDAR aeronomical community to have measurements of the line shape profile of the OI (5577 Å) emission during the September, 1987, LTCS campaign. The filter used has a bandwidth of 3 Å centered slightly above the green line peak wavelength. Tilting the filter fine tunes the Fabry Perot's response to the sky emission. The filter remains in use in Thule along with the OI (6300 Å) filter necessitating a bi-filter scanning sequence. At each pointing direction, first a green line fringe is acquired and then a red line fringe before moving the mirror system to a new direction. With the new OI (6300 Å) filter mentioned above, a full scan including the lower thermosphere measurements as well as the dark and Ne experiments requires on the average 20 minutes.

The 0.5m Ebert Fastie spectrophotometer has been operating at the Thule site during the period of this report. Prior to the summer of 1989, the instrument was interfaced to the same data acquisition computer as the Fabry Perot interferometer and used the same data control crate. The instrument is pointed at the zenith which, in Thule, is approximately the geomagnetic zenith direction. The detector is a GaAs photomultiplier tube which has a relatively high quantum efficiency in the first order wavelength coverage of the spectrophotometer - ~3800 to ~7600 Å. The instrument routinely monitors several nightglow emissions as well as the scattering from low altitude clouds or fog from base lighting. During attended operation, wavelength and intensity calibrations are routinely performed. A set of spectral lamps permits wavelength calibration while a calibrated intensity source allows intensity calibration. This source has been characterized many times during its lifetime, most recently in September, 1987. The source has a peak response near 6300 Å of 7 R/Å and may be used to intensity calibrate the spectrophotometer over its full range of sensitivity. In addition, while an operator is present, the intensity calibration is transferred to the Fabry Perot interferometer by pointing the latter instrument at the zenith. Knowledge of the filter transmission functions plus the results of the cross calibration experiments allows a reasonable estimate as to the true brightness of the nightglow viewed by the Fabry Perot interferometer.

In an effort to increase the efficiency of the the spectrophotometer experiment, the instrument was interfaced with an IBM AT clone computer during the 1989 down season. This was accomplished at SPRL by two students funded by the REU program. The ra-

tionale for this major change was twofold: one, to make the experiments in Thule truly independent; and two, to upgrade the computer control system to current state of the art levels. The upgrade was motivated by the successes that were made during the startup efforts in September, 1987, and November, 1988. Both the Fabry Perot interferometer and the Ebert Fastie spectrophotometer experiments performed so well that the single data acquisition computer became overloaded with data prior to a site visit and, as a result, shut down for lack of disk space. Rather than increasing disk space on the old PDP 11/23 computer, weaning the spectrophotometer experiment away from this computer and interfacing with its own system with an optical disk drive data storage unit was the preferred solution. This new arrangement was tested in Ann Arbor in September, 1989, and was shipped and installed at Thule Air Base in November, 1989.

During the fall of 1987, an additional trailer was placed next to the original Wells Fargo trailer. The new trailer initially had one hole cut into the ceiling with a clear Plexiglass dome placed over it. In November, 1988, an all sky camera system was placed under this dome. The detection system for this experiment makes use of a bare CCD placed at the focal plane of an all sky camera lens system. The filter wheel with its complement of filters was placed above the input optics. Since it was decided at the very start that there would not be any image intensification, the CCD must be kept as cold as possible to reduce the dark count inherent within the device. This is accomplished in several ways. First of all, the trailer housing this experiment is kept at ambient temperature which is near -30°C during the winter months. Secondly, the Peltier cooling system that was supplied by the vendor was supplemented with a thermoelectric cooling system. Dark counts were observed to be as low as 5 counts per 300 seconds. The current version of the experiment is capable of imaging sub-visual auroral arcs and patches at 5577 and 6300 Å. The images are recorded on video tape for playback and analysis in Michigan.

During the fall of 1990, a Michelson interferometer was placed under a new second dome in the second trailer. The instrument is controlled by a separate computer and runs independently of the three other experiments. The bandwidth observed by the Michelson interferometer is the near infrared from 10000Å to 16000Å which includes many intense hydroxyl airglow emissions as well as two bands of the near infrared O_2 IR Atmospheric band. The instrument was setup to obtain two minute integration spectra during twilight and ten minute integrations during dark conditions. Figure 2 shows an example of a reduced data set for one night at Thule Air Base. The top half shows a time series of mesopause neutral temperatures extracted from the Meinel OH (3,1) band. The bottom half shows the corresponding time series of intensity variations.

RESULTS

The Thule Air Base facility was brought on line in November, 1989 by Dr. Niciejewski and graduate students Matt Turnbull and Elaine Trudell. Dr. Niciejewski initiated the FPI and led the effort, Mr. Turnbull initiated the EFS, while Ms. Trudell initiated the all-sky camera system operation. The site was again visited by Dr. Niciejewski in February, 1990 to back up data sets as well as to fix a software problem with the EFS. Mr. Turnbull was charged with shutting down the station for the summer term as well as returning the all-sky camera to Michigan during a visit in April, 1990. The site was next visited by Andy Berki during August, 1990 to perform modifications to the second trailer. The 1990/1 observing season was initiated by a visit in September, 1990, by Mr. Turnbull and Drs. Niciejewski and Murty. During that trip, a Michelson interferometer was added to the instrumental complement. Unfortunately, the photomultiplier tube for the EFS did not function so the EFS was not brought on line at that time. The site was visited by Dr. Murty in December, 1990 to back up old FPI and MI data. The site was next visited by Dr. Niciejewski, Capt. Stephen Carr, and Ms. Trudell in January, 1991. The EFS was repaired and placed in operation for the rest of the season. Ms. Trudell was charged with installing the all-sky camera experiment. Unfortunately, one box of the shipment did not arrive on time which meant that this experiment did not operate during that season. Dr. Killeen visited the site in February, 1991, to back up old data sets. Shutdown was performed in April, 1991, by Capt. Carr, who also returned the MI and the all-sky camera boxes to Michigan.

During the periods mentioned above, high quality data were acquired by the FPI between January, 1990 and February, 1990; January, 1991 and February, 1991. The EFS acquired data between February, 1990 and March, 1990; January, 1991 and March, 1991. The MI acquired data between January, 1991 and March, 1991. Cloud cover records have been acquired from the Thule Air Base meteorological station. Much of the Fabry Perot interferometer data and all the cloud cover records have been entered into an "in house" data base at SPRL. Figure 3 shows some results obtained from the data base. The average horizontal neutral wind meridional and zonal components at F region altitudes are shown for conditions where $K_p \leq 3$ (top) and $3 < K_p < 6$ (bottom). Figure 4 displays averaged components for E region altitudes.

Several papers resulting from the analysis of Thule Fabry Perot interferometer data have been published during this report interval. The first paper [Killeen *et al.*, 1991] was the result of a contribution to an IUGG conference and described Thule Air Base measurements in the context of other high latitude measurements. The second paper [Niciejewski *et al.*, 1992] described the effect of the orientation of the B_y component of the IMF on neutral winds at high latitudes. The third paper [Niciejewski and Killeen, 1992] described the effect of K_p on the magnitude of the high latitude meridional neutral wind flow and described the appearance of midnight abatement features in response to extremely low K_p conditions. The fourth paper [Niciejewski *et al.*, 1993] described observations of neutral winds in the presence of sun-aligned auroral arcs above Thule Air Base. This paper is currently undergoing revision. The fifth paper [Thayer *et al.*, 1994] described an experimental ground-based measurement of the ion/neutral coupling at very high geomagnetic latitudes. The sixth paper [Johnson *et al.*, 1994] described observations and model predictions of neutral winds during the January, 1988 GISMOS experimental period. The seventh paper [Niciejewski *et al.*, 1994] described the effect of the orientation of the B_z component of the IMF on neutral winds at high latitudes.

Many presentations at scientific conferences have been made during the report period which include data sets obtained at the Thule Air Base optical facility. One paper was

presented at the Fall '89 AGU meeting. Three papers were presented at the Spring '90 AGU meeting. One paper was presented at the COSPAR '90 meeting. One paper was presented at the Spring '91 AGU meeting. One paper was presented at the URSI '91 meeting. Three papers were presented at the IUGG '91 meeting. One paper was presented at the Fall '91 AGU meeting. Two papers were presented at the Spring '92 AGU meeting. One paper was presented at the COSPAR '92 meeting. Three papers were presented at the 1992 AGU Chapman conference. Two papers were presented at the Spring '93 AGU conference.

The facility at Thule Air Base has been used to train graduate students in the operation and maintenance of ground based optical instrumentation. During the period of this report, the station has been visited by Mr. M. Turnbull, Capt. S. Carr, and Ms. E. Trudell. In addition, Mr. D. Drob and Mr. Y. Won have been involved in the data analysis and interpretation of Thule data. Mr. J. Thayer, Mr. Y. Won, and Capt. S. Carr have completed PhD degrees using data sets accumulated at Thule Air Base. Mr. Drob and Ms. Trudell are completing their graduate degree requirements using data obtained from the Thule site, the former using MI and FPI data, the latter using FPI and all-sky camera data.

SUMMARY

A computer controlled, automatic airglow facility has been in operation at Thule Air Base during the winter observing periods covered by this report. The instrumentation complement includes a Fabry Perot interferometer monitoring thermospheric emissions from OI (5577 Å) and OI (6300 Å), a spectrophotometer monitoring airglow emissions, an all sky imaging system monitoring visual to sub-visual auroral arcs and patches, and a near infrared Fourier transform spectrometer monitoring hydroxyl emissions. Thermospheric neutral winds and temperatures have been measured routinely since 1985 leading to an initial description of polar cap thermodynamics during the solar minimum and solar maximum phases.

REFERENCES

- Killeen, T. L., F. G. McCormac, A. G. Burns, J. P. Thayer, R. M. Johnson, and R. J. Niciejewski, On the dynamics and composition of the high-latitude thermosphere, *J. Atmos. Terr. Phys.*, 53, 797, 1991.
- Niciejewski, R. J., T. L. Killeen, R. M. Johnson, and J. P. Thayer, The behavior of the high-latitude F-region neutral thermosphere in relation to IMF parameters, *Adv. Space Res.*, 12, (6)215, 1992.
- Niciejewski, R. J., and T. L. Killeen, Thermospheric wind measurements from Greenland: the midnight abatement feature, submitted to *Advances in Space Research*, 1992.
- Niciejewski, R. J., T. L. Killeen, and E. Trudell, OI (6300 Å) observations in the high latitude thermosphere during dynamic events, submitted to *Radio Science*, 1993.
- Thayer, J. P., R. J. Niciejewski, T. L. Killeen, J. Buchau, B. W. Reinisch, and G. Crowley, Ground-based observations of ion/neutral coupling at Thule and Qanâq, Greenland: IMF B_z dependence, in preparation, 1994.
- Johnson, R. M., J. Thayer, R. J. Niciejewski, R. G. Roble, B. Emery, M. Buonsanto, D. Knipp, O. de la Beaujardière, and T. L. Killeen, High-latitude convection and meridional winds during the January 1988 GISMOS: Observations and thermosphere ionosphere general circulation model results, in preparation, 1994.
- Niciejewski, R. J., T. L. Killeen, and Y. Won, Observations of neutral winds in the polar cap during northward IMF, *J. Atmos. Terr. Phys.*, 56, 285, 1994.

FIGURE CAPTIONS

Figure 1. The Thule optical facility consists of two instrumented trailers for scientific research. The trailer in the foreground on the left houses the Fabry Perot interferometer and Ebert Fastie spectrophotometer. The trailer on the right houses the all sky camera system and the Michelson interferometer, the former under a small dome not seen in the photograph.

Figure 2. Summary plot of mesopause data for the date 09/24/90 as acquired by the Thule Air Base Michelson interferometer experiment. The top figure displays a time series of neutral temperatures as derived from a series of Meinel OH (3,1) band spectra. The bottom figure displays the corresponding OH intensity time series.

Figure 3. Component plot of averaged meridional and zonal neutral winds in the upper thermosphere as observed over Thule Air Base for conditions of $K_p \leq 3$ (top) and $3 < K_p < 6$ (bottom).

Figure 4. Component plot of averaged meridional and zonal neutral winds in the lower thermosphere as observed over Thule Air Base for the winter of 1988/89 (top) and the winter of 1990/91 (bottom).

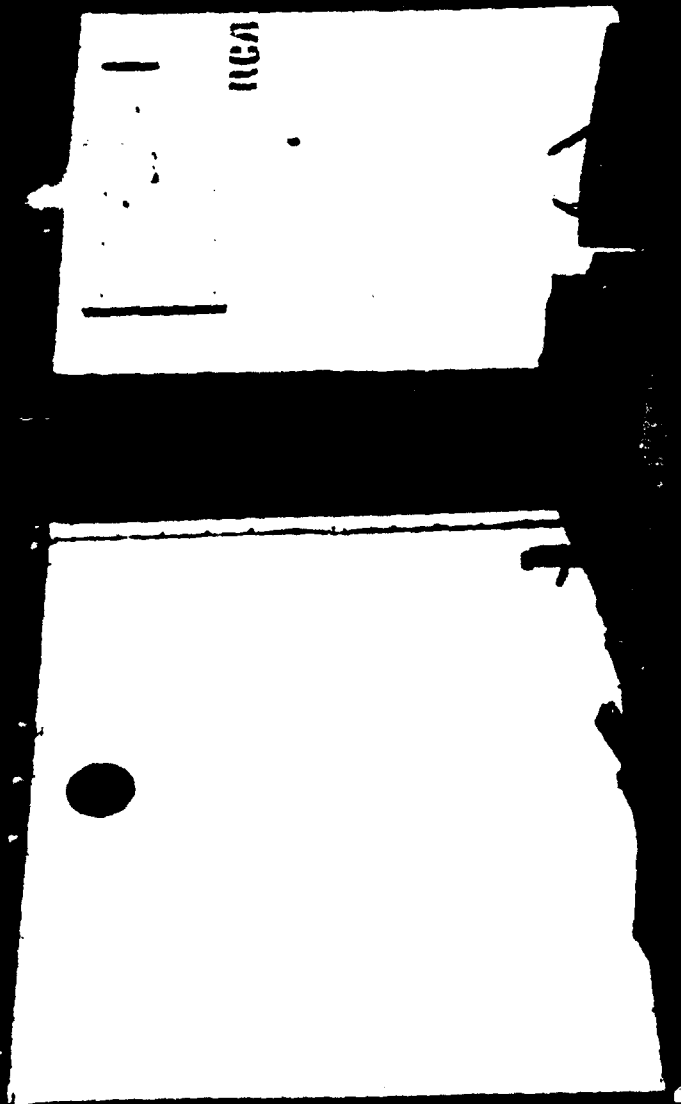


FIGURE 1

Thule Air Base 092490

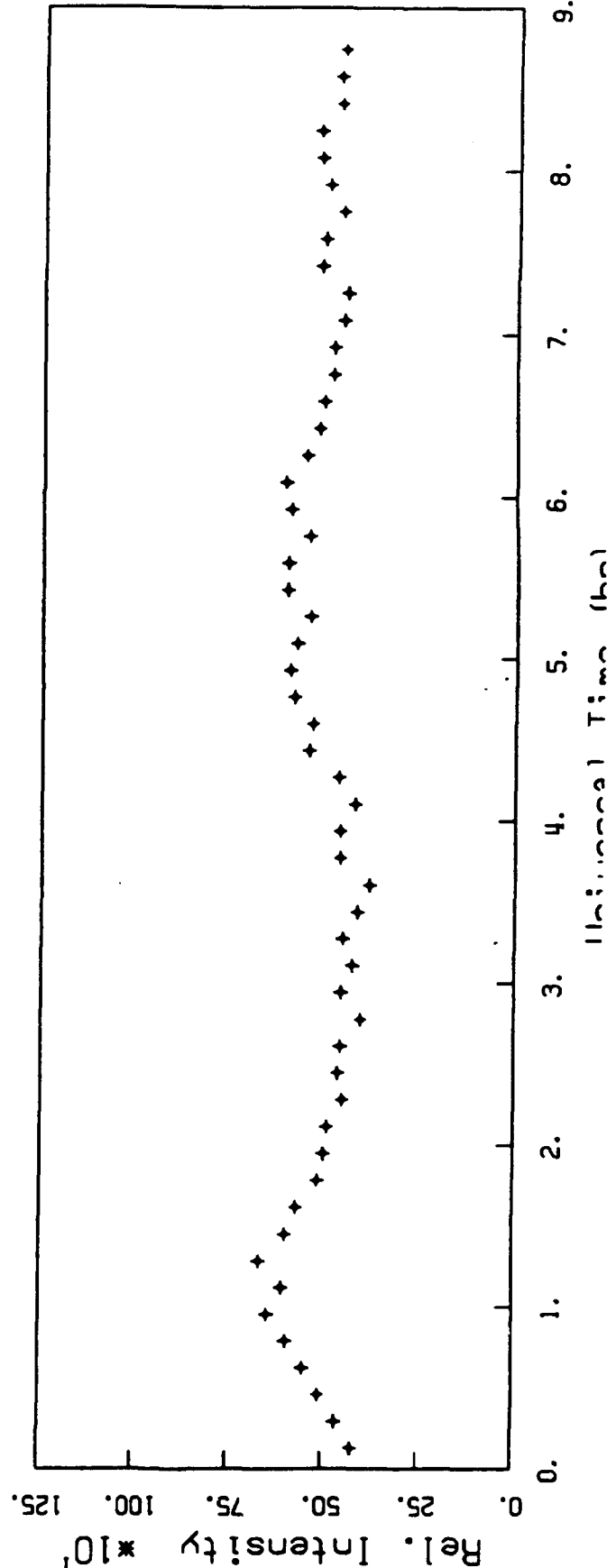
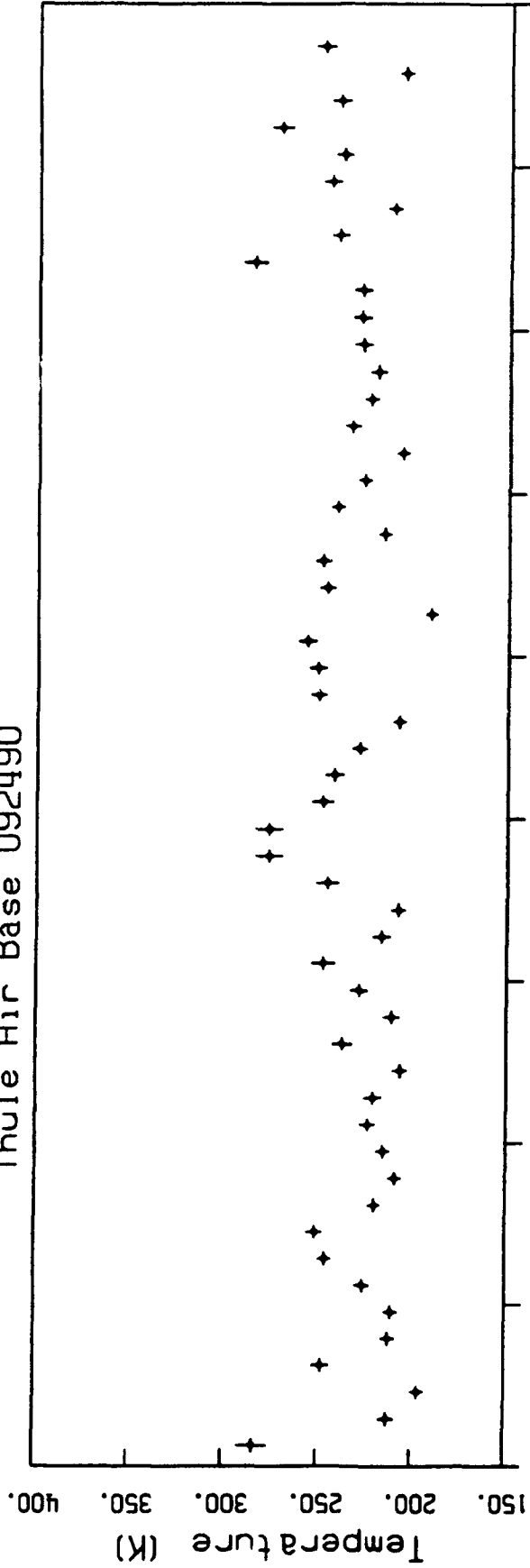


FIGURE 2
10

AVERAGE HORIZONTAL WIND COMPONENTS OVER THULE, GREENLAND

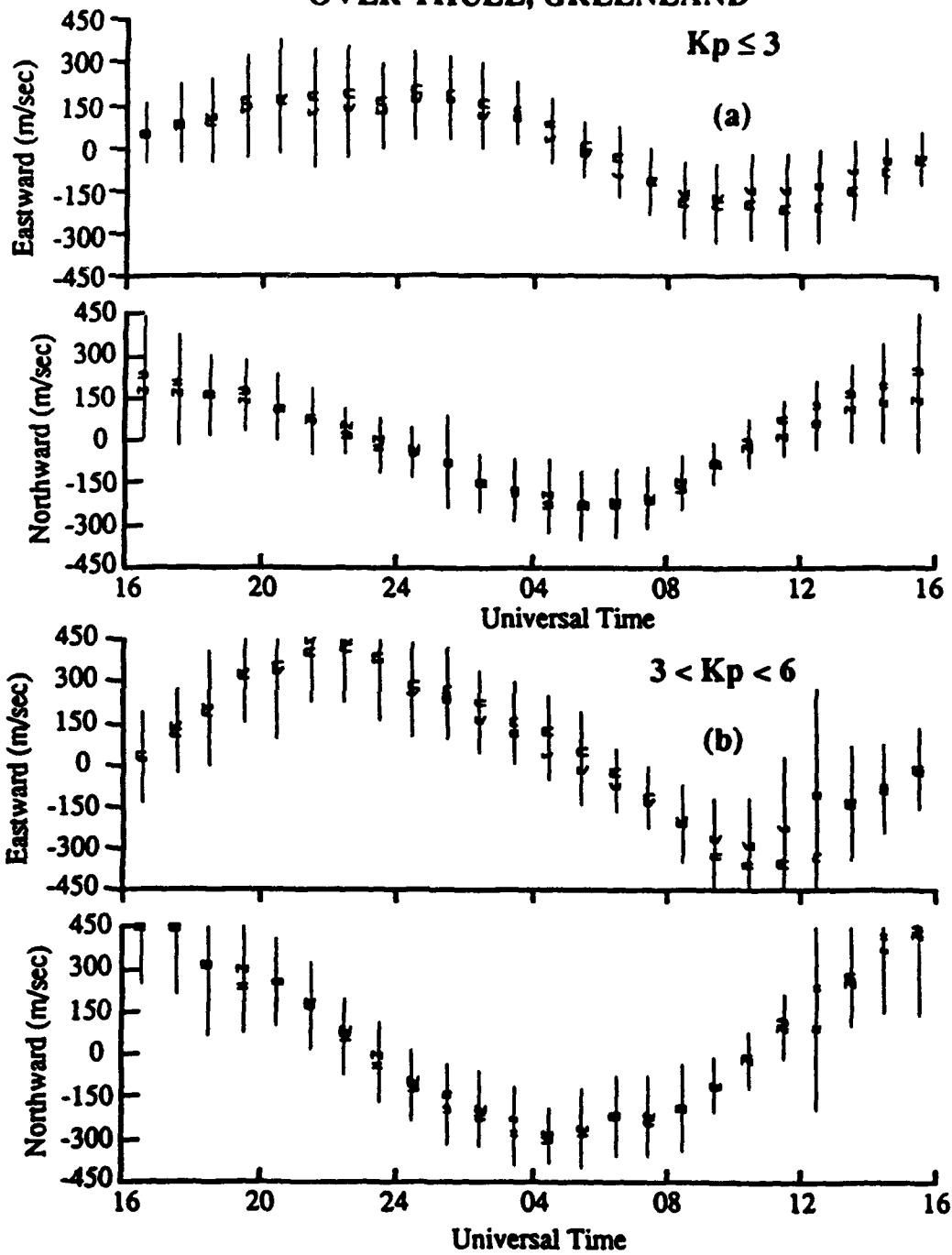


FIGURE 3

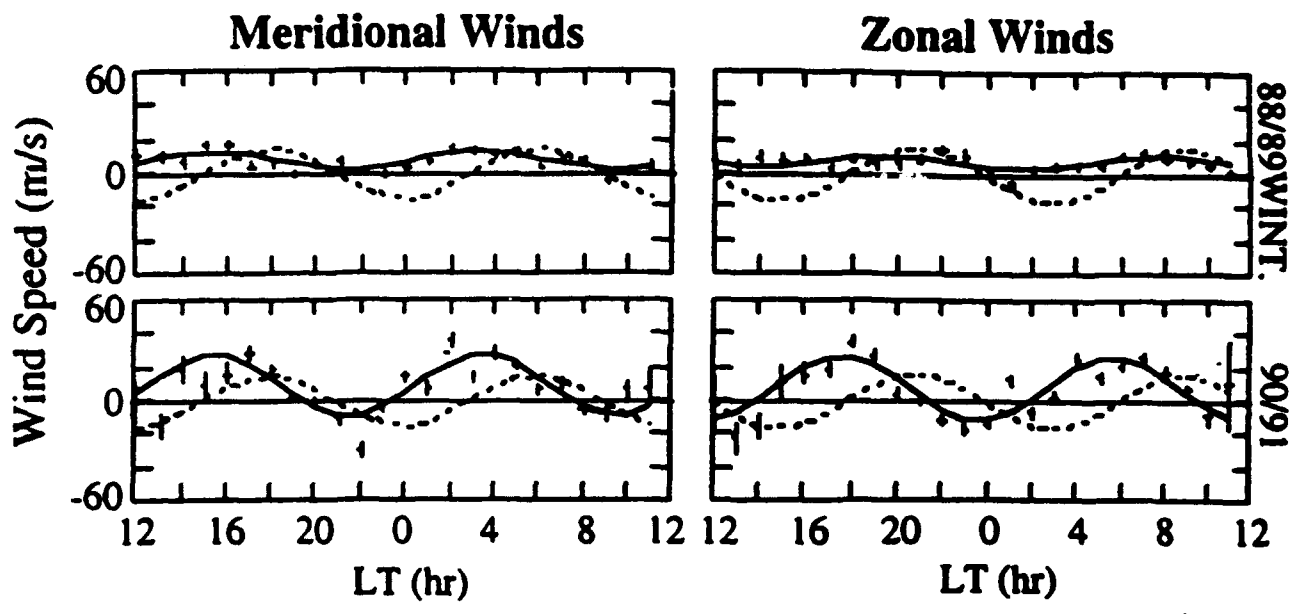


FIGURE 4

APPENDIX A

On the dynamics and composition of the high-latitude thermosphere

T. L. KILLEEN, F. G. McCORMAC,* A. G. BURNS, J. P. THAYER,†
R. M. JOHNSON and R. J. NICIEJEWSKI

Space Physics Research Laboratory, Department of Atmospheric, Oceanic and Space Sciences,
The University of Michigan, Ann Arbor, MI 48109, U.S.A.

(Received in final form 3 April 1991)

Abstract—Recent experimental measurements of the dynamics of the neutral upper thermosphere have demonstrated the important roles of ion-drag and Joule heating processes in establishing the basic neutral wind morphology and controlling neutral composition, particularly in the high-latitude region. Instruments on the Dynamics Explorer-2 spacecraft (DE 2), for example, were capable of measuring the three-dimensional vector neutral wind and ion drift in the thermosphere along the orbital track, together with constituent densities and temperatures. Ground-based optical and radar measurements of winds and temperatures from observatories in Greenland have contributed additional measurements of thermospheric neutral wind velocities and ionospheric parameters. The comprehensive nature of these various data sets has enabled more stringent experimental constraints to be placed on the numerical models of the region (thermosphere-ionosphere general circulation models, TIGCMs), leading to an improved theoretical understanding of the important physical processes that control thermospheric circulation and variability. In addition, the measurements have enabled the development of semi-empirical models of thermosphere dynamics which can be used in various theoretical studies. The Vector Spherical Harmonic (VSH) model, for example, provides a description of global thermospheric state variables (wind, temperature and density), using a combination of empirical data and NCAR-TIGCM calculations. This paper presents a brief review of some of the more recent progress made in this area by the team of researchers at the University of Michigan, with emphasis on the interpretation of experimental measurements made from DE 2 and from ground-based observatories in Thule and Søndrestørmfjord, Greenland. Comparisons between individual data sets from these sources and the VSH model are also presented.

1. INTRODUCTION

The dynamics, thermodynamics, and compositional structure of the neutral gas in the upper thermosphere are strongly controlled by ion-neutral collision processes, particularly at high geomagnetic latitudes. Magnetospheric convection electric fields map down into the high-latitude ionosphere along equipotential geomagnetic field lines and drive the charged particles there into cellular motion. Rapidly moving ions in these ionospheric convection cells can readily transfer momentum to the neutral gas via ion-drag forcing and can convert a portion of their kinetic energy of motion into internal energy of the neutral gas via Joule or collisional heating. In addition, the enhanced concentrations of ions associated with auroral particle precipitation serve to increase the rates of exchange of energy and momentum between the neutral and ionized species by increasing the magnitude of the ion-

neutral collision frequency amongst other factors. The effect of these high-latitude ion-neutral collision processes is to modify the neutral wind, temperature and compositional structure away from the structure that would be expected if the only sources of energy for the thermosphere were solar UV and EUV insolation.

Many examples of the effects of auroral/magnetospheric forcing of the neutral thermosphere at high latitudes have been reported in the literature over the past 10 years (e.g. see the review articles of MERIWETHER, 1983; ROBLE, 1983; MAYR *et al.*, 1985; KILLEEN, 1987; KILLEEN and ROBLE, 1988). Rapid experimental and theoretical progress has been sustained due, in part, to the comprehensive nature of new data sets provided by the NASA Dynamics Explorer-2 spacecraft (DE 2) and the ground-based network of optical interferometer observatories and incoherent scatter radar facilities, as well as to the maturity of the numerical, three-dimensional, time-dependent, thermosphere/ionosphere general circulation models (TIGCMs). The two best-developed examples of the latter are the National Center for Atmospheric Research model (NCAR-TIGCM) of DICKINSON *et al.* (1981) and ROBLE *et al.* (1982,

* Now at The Radiocarbon Laboratory, Queens University, Belfast, U.K.

† Now at The Geoscience and Engineering Center, SRI International, 333 Ravenswood Avenue, Menlo Park, CA 94025, U.S.A.

1988) and the University College London/Sheffield University model of FULLER-ROWELL and REES (1980) and FULLER-ROWELL *et al.* (1987). Two semi-empirical models of neutral thermosphere dynamics have also been developed in recent years, the Vector Spherical Harmonic (VSH) model of KILLEEN *et al.* (1987) and the Horizontal Wind Model (HWM) of HEDIN *et al.* (1988, 1991). While the HWM model is entirely based on observations, the VSH model is a hybrid, based primarily on the theoretical calculations from the NCAR-TIGCM, but supplemented with DE 2 measurements where available.

In this paper, we summarize some of the recent high-latitude results obtained using the DE 2 thermospheric neutral wind, temperature and composition data, together with VSH model predictions. Additional experimental results from ground-based optical observatories sited at Thule and Sondrestromfjord (Sondrestrom), Greenland and from the incoherent scatter radar at Sondrestrom are also shown. The emphasis of this discussion is on perturbations to the solar-driven upper thermospheric winds, temperatures and compositional structures due to forcing associated with high-latitude ionosphere-thermosphere coupling processes. In the following sections we (1) discuss the nature of the experimental measurements made on the DE 2 spacecraft and describe some recent results, (2) describe briefly the VSH model, some sample results, and experiment-model comparisons using both satellite and ground-based measurements of high-latitude thermosphere dynamics, (3) discuss considerations pertaining to compositional perturbations at high latitudes, and (4) make some concluding remarks.

2. DYNAMICS EXPLORER MEASUREMENTS

The Dynamics Explorer-2 spacecraft payload included the Fabry-Perot interferometer, FPI (HAYS *et al.*, 1981), the Wind and Temperature Spectrometer, WATS (SPENCER *et al.*, 1981), and the Neutral Atmosphere Composition Spectrometer, NACS (CARIGNAN *et al.*, 1981). These instruments measured the meridional and zonal components of the neutral wind and neutral constituent abundances, respectively, along the track of the polar-orbiting satellite. Both the FPI and WATS instruments also measured neutral kinetic temperatures. In addition to these instruments, the Langmuir probe, LANG (KREHBIEL *et al.*, 1981), the Ion Drift Meter, IDM (HEELIS *et al.*, 1981), and the Retarding Potential Analyzer, RPA (HANSON *et al.*, 1981) measured the ion density and the zonal meridional components of the ion drift, respectively. The RPA and LANG

instruments also enabled measurements of ion and electron temperatures, respectively. The comprehensive nature of the DE 2 data set has enabled various studies of thermospheric ion-neutral coupling at high latitudes to be conducted (see the review by KILLEEN and ROBLE, 1988).

Examples of the DE 2 coverage for two nearly full orbits of the spacecraft are shown in Figs 1 and 2. These figures show, as a function of various geophysical parameters along the orbital track of the spacecraft, the following measured or derived observables (from top to bottom): (1) the neutral wind vector from FPI and WATS; (2) the ion drift vector from IDM and RPA; (3) the atomic oxygen, molecular nitrogen and electron number densities from NACS and LANG, respectively; (4) the electron, ion, and neutral kinetic temperatures from LANG, RPA and FPI, respectively; and (5) vertical winds and ion drifts measured from WATS and IDM, respectively. The upper inset to the left of each figure is a dial showing the neutral winds (Fig. 2) or ion winds (Fig. 1) in a geographic polar projection for the southern hemisphere. The lower inset provides information on the time history of the relevant interplanetary magnetic field (IMF) components and the K_p and AE geomagnetic indices prior to and at the time (given by the dotted vertical line) of the orbital pass. The vectors are plotted such that local noon is to the top of the diagram and local dawn to the right. Thus, the downward-directed ion drift vectors are in the anti-sunward direction and are generally associated with the central region of the northern and southern hemisphere geomagnetic polar caps, while the regions of upward-directed ion drift vectors are in the sunward direction and are generally associated with the dawn and dusk sectors of the auroral zones.

Figure 1 presents data from orbit 7366 of DE 2 which occurred during Julian day 82338. As can be seen from the lower inset, this orbit occurred during relatively quiet geomagnetic conditions, with $K_p = 1$ ($A_p = 13$). By contrast, Fig. 2 shows data from orbit 7219 on day 82328 which was a period of intense geomagnetic activity, with $K_p = 7$ ($A_p = 83$). In both cases, the satellite obtained data across both northern (winter) and southern (summer) high-latitude regions, as well as low- and mid-latitudes. These data are shown to provide an overview of the variations in thermospheric state variables typically observed from DE 2.

There are several general features that can be discerned from Figs 1 and 2. Most obviously, the neutral and ion winds (including the horizontal and vertical components) have their greatest structure and magnitudes in the two polar regions, with clear evidence

DE-2 FPI/WATS/RPA/IDM/NACS/LANG

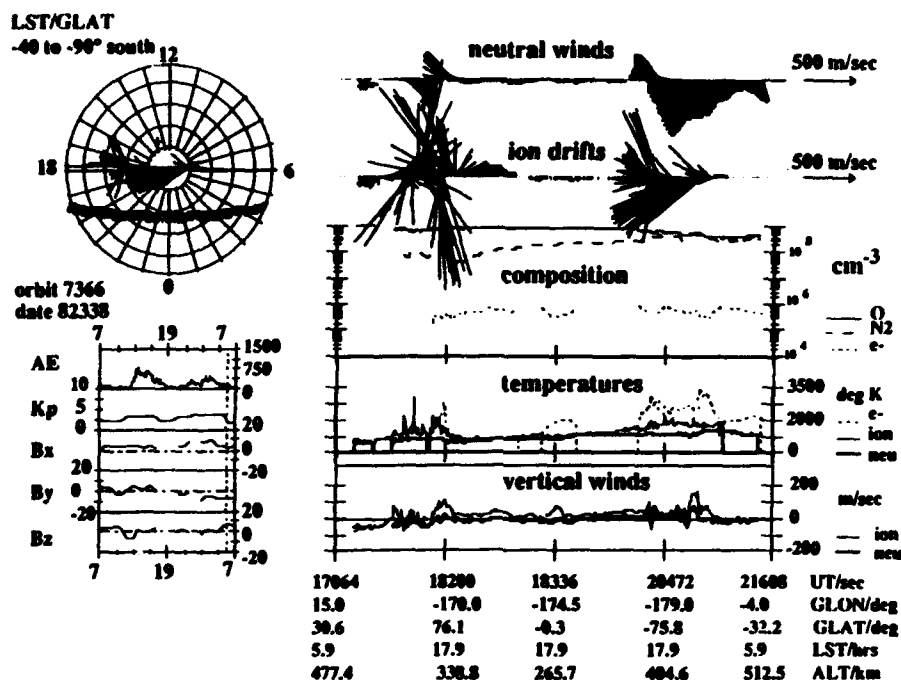


Fig. 1. Geophysical observables measured along the track of Dynamics Explorer 2 during orbit 7366. The neutral winds and ion drifts are shown in the top two traces plotted against time, altitude, and latitude of the spacecraft as it successively passes (left-to-right) over the northern hemisphere (winter) polar region, the equatorial region and the southern hemisphere (summer) polar region. The second panel shows the atomic oxygen and molecular nitrogen densities, referred to a fiducial altitude of 300 km, and the electron (ion) density. The third panel shows the electron (dotted line), ion (light line) and neutral (bold line) temperatures measured along the orbital track. The bottom trace shows the measured vertical neutral winds (bold line) and ion drifts (light line). The lower inset to the left shows the time history of the IMF components and the geophysical indices AE and K_p for the 24 h prior to the orbital pass. The mid-point UT for the satellite pass is denoted by the vertical dotted line. The upper inset to the left shows a polar dial (geographic latitude and solar local time) for the pass, with the ion winds plotted and the location of the geomagnetic pole given by the cross.

of a predominantly two-cell ion convection pattern and a morphologically similar, but less strong, neutral wind system at high latitudes. The neutral winds (and ion drifts) at mid- and low-latitudes (central region of figures) have much smaller magnitudes and are consistent with a day-to-night solar-driven global thermospheric wind system. The neutral composition measurements obtained during these passes have all been adjusted to an altitude of 300 km in order to highlight latitudinal rather than altitudinal changes, using a diffusive equilibrium approximation to map the measured values upwards or downwards from the corresponding spacecraft altitude for each measurement. The $[O]$ and $[N_2]$ densities, referred to 300 km altitude, show relatively smooth and unstructured behavior at mid- and low-latitudes, and more struc-

tured perturbations at polar latitudes, in response to the temporally and spatially complex high-latitude ion drag and Joule heating processes. For both the quiet-time orbit (7366) and the active-time orbit (7219), the N_2 densities at 300 km equal or exceed the corresponding O densities in the summer hemisphere polar regions due to the extra heating and consequent upwelling of the thermosphere. The O densities do not show the strong summer-to-winter gradient observed in the N_2 densities for the active period and, in fact, show decreases at high latitudes during the disturbance when N_2 increases. These 'anomalies' are well understood and are related to the different masses of the species. It is also interesting to note that the vertical velocities tend to be more upwards in the warmer summer hemisphere and in regions of

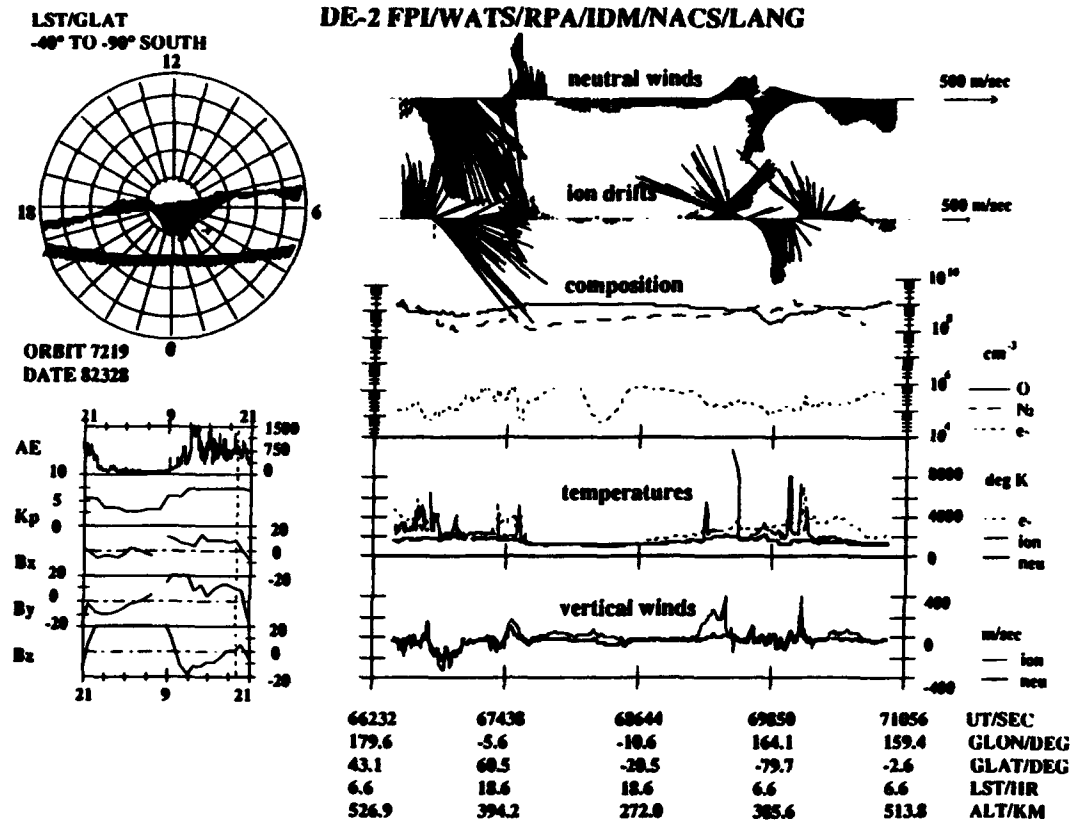


Fig. 2. Geophysical observables measured along the track of Dynamics Explorer 2 during orbit 7219. The format of the figure is as for Fig. 1, with the exception that neutral winds rather than ion drifts are shown in the polar dial to the upper left.

enhanced auroral heating. The electron density (n_e) measurements show various structures associated with ionospheric morphology. A particular feature of interest occurs near 68200 s UT, where a depression in n_e at equatorial latitudes is probably an altitude effect caused by the relatively high F_2 -region peak and the relatively low satellite altitude; in this region the satellite dips below the F_2 peak. The vertical wind measurements (bottom panel) show evidence for the presence of gravity wave activity at polar latitudes with various horizontal wavelengths, ranging from a few degrees to tens of degrees in latitude.

The measured ion, electron and neutral temperatures (T_i , T_e and T_n , respectively) along the orbital tracks provide insight into the thermal structure of the upper atmosphere. As expected, the magnitude of T_e is the greatest of the three, except for localized regions of very strong Joule heating where T_i can exceed T_n . Such a period occurred during the southern

hemisphere polar passage for orbit 7219, where the greatly enhanced frictional heating of the ions, due to the large ion-neutral difference velocities, caused localized enhancements in ion temperature to many thousands of degrees. In general, all three species are in thermal equilibrium at low latitudes ($T_e \approx T_i \approx T_n$), with major departures from that equilibrium occurring at high latitudes.

The effects of enhanced levels of geomagnetic activity can be seen by comparing the data of Fig. 1 and Fig. 2. The neutral and ion winds, neutral densities, and neutral and ion temperatures are typically all greater in magnitude during the more geomagnetically active orbit 7219 than during orbit 7366. Neutral winds in excess of 1200 m/s were observed near 67400 s UT on orbit 7219, which occurred during an extended period of greatly enhanced geomagnetic activity (see, for example, the AE trace in the lower inset of Fig. 2). These are the largest magnitude winds observed by DE and it is our belief that these are the

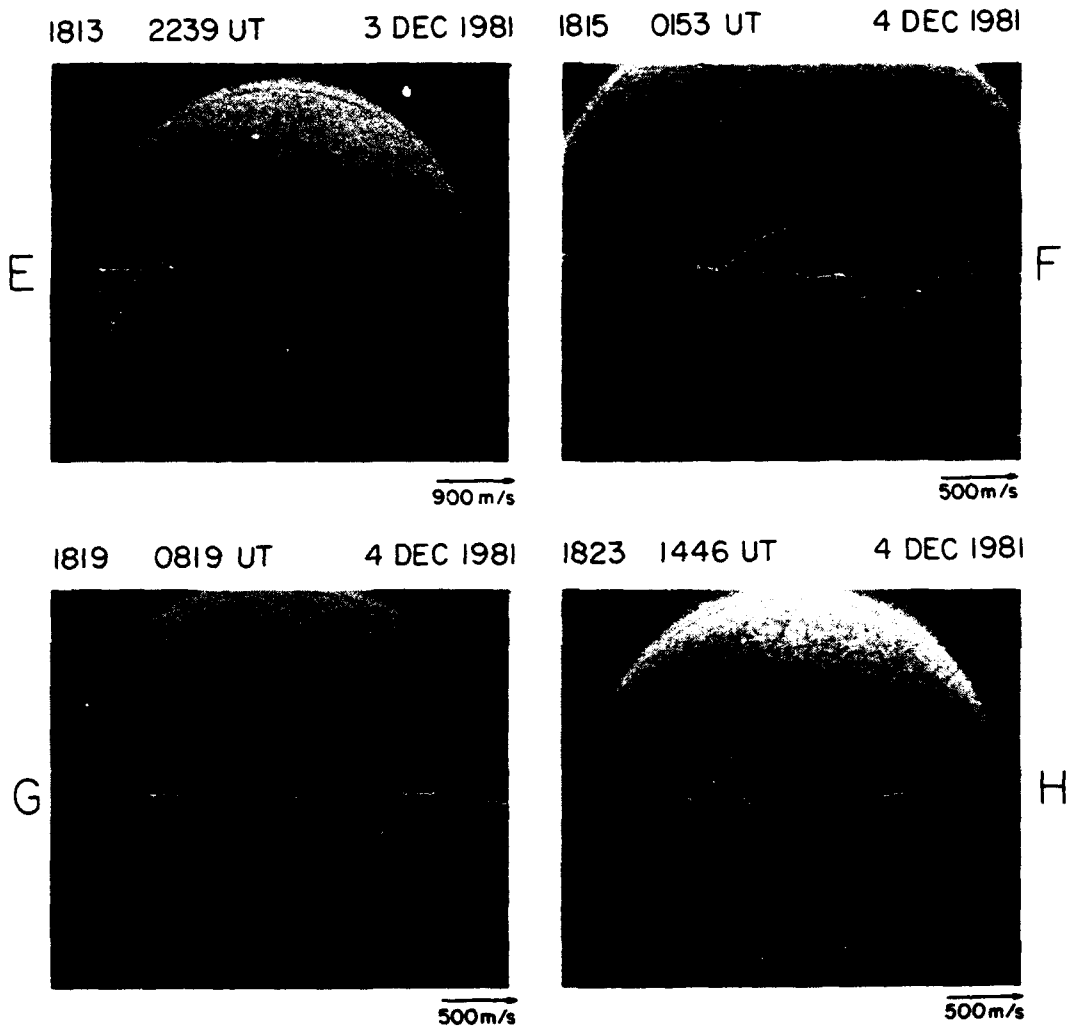


Fig. 3. Simultaneously measured neutral wind vectors from DE2 (orbit 1813) and DE1 auroral image (courtesy of L. A. Frank and J. D. Craven, University of Iowa). The images were obtained using the Spin-Scan Auroral Imager, SAI, on Dynamics Explorer 1, viewing the northern hemisphere aurorae at ultraviolet wavelengths. The images are false-color coded and are oriented such that the direction towards the Sun is to the top of the figure, dusk to the left. The solar terminator is evident, running roughly horizontal across each image, as is the entire auroral oval located just to the nightside of the terminator. The neutral wind vectors are denoted by the yellow arrows whose origins are positioned along the DE 2 orbital track. The wind scale is given at lower right. 3b-d are for DE 2 orbits 1815, 1819 and 1823, respectively. The figure is taken from KILLEEN *et al.* (1988).

DE 2 FPI/WATS/IDM/RPA DAY 82328

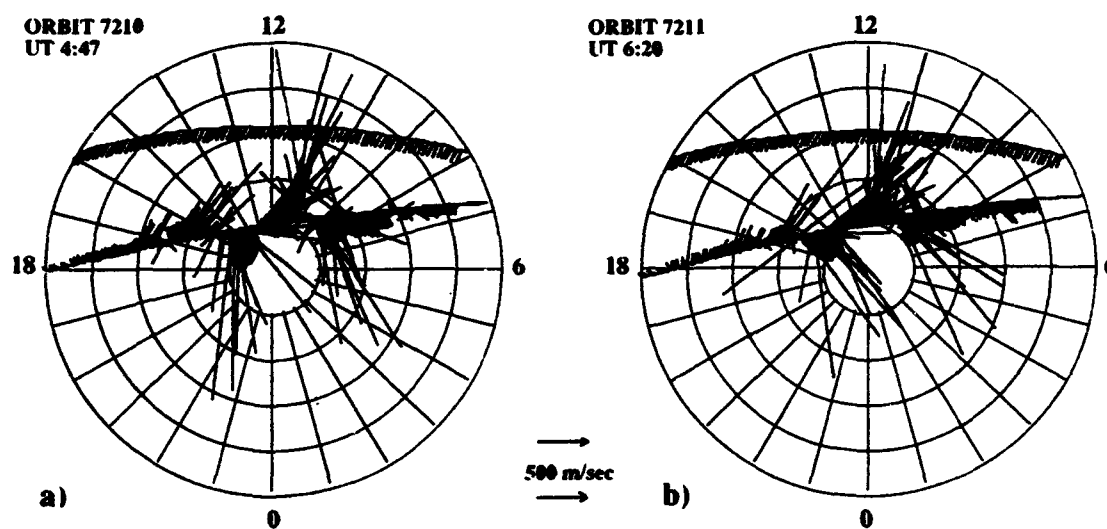


Fig. 7. Neutral winds and ion drift measurements (blue arrows and red bars, respectively) are plotted along the orbital track of Dynamics Explorer 2 during orbits 7210 and 7211. The data are plotted in geomagnetic polar coordinates (magnetic local time and magnetic latitude), with the outer circle being at 40° geomagnetic. These data were obtained during a prolonged period of strongly northward IMF. The figure is adapted from KILLEEN *et al.* (1985).

Neutral Winds and Temperatures

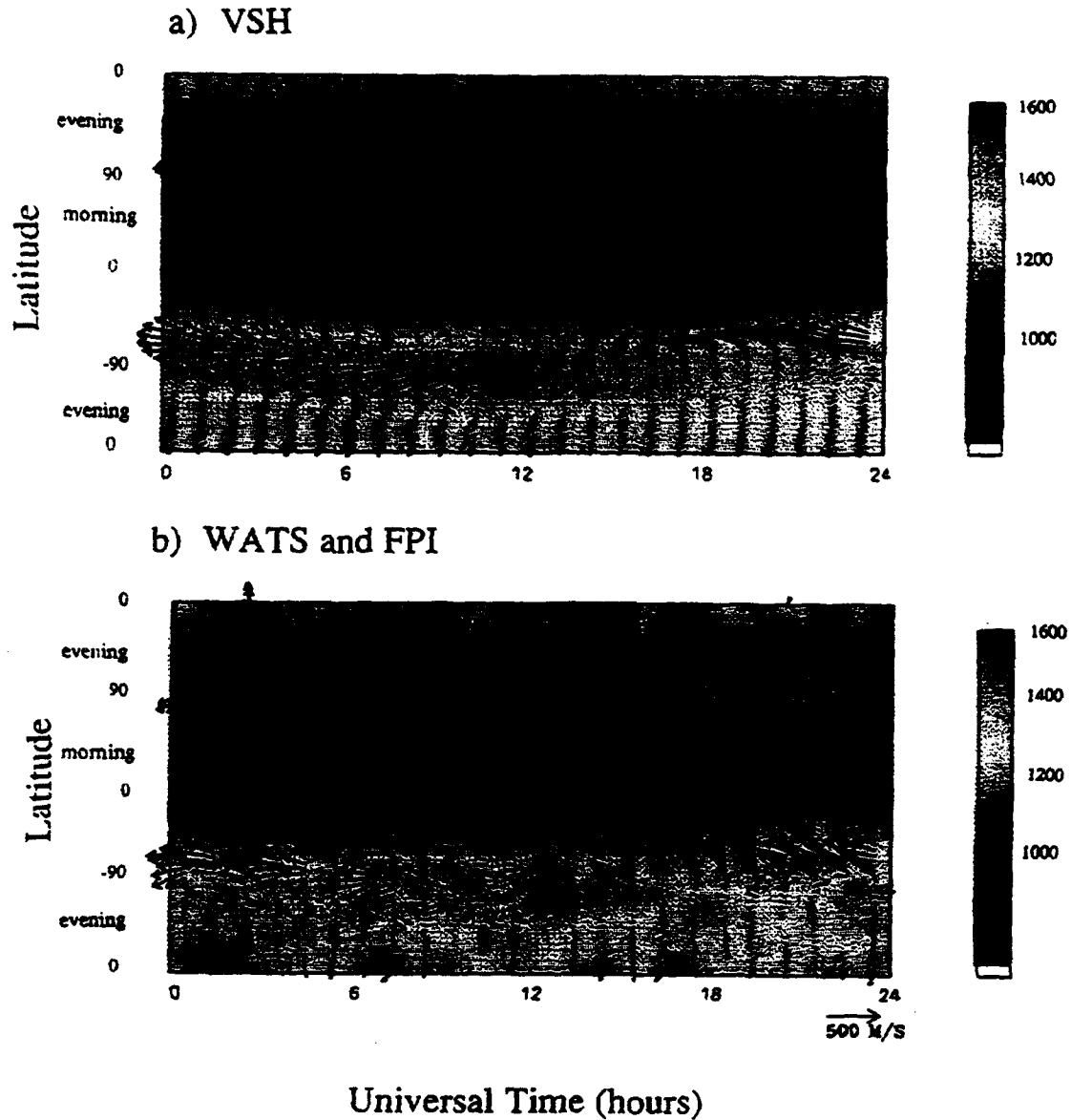


Fig. 10. Thermospheric wind and temperature plots for December solstice solar maximum conditions. (a) VSH model predictions; (b) averaged DE 2 winds and temperatures collected between November 1981 and January 1982 and between November 1982 and January 1983. The plots are in geographic latitude and Universal Time.

largest magnitude winds yet reported for any part of the Earth's atmosphere.

While the study of thermospheric and ionospheric parameters from individual high-latitude orbital passes provides information on the response of the upper atmosphere to energy and momentum inputs from the magnetosphere, the study by KILLEEN *et al.* (1988) illustrated unambiguously the relationship between thermospheric winds and one of the most obvious manifestations of magnetospheric processes—the visible aurora. Figure 3 shows simultaneous measurements of global-scale auroral luminosity distributions and vector neutral winds over the northern (winter) polar cap, using data from the spin-scan auroral imager, SAI (FRANK *et al.*, 1981), on DE 1 and the FPI and WATS instruments on DE 2, respectively. This work illustrates the spatial relationship between large-scale morphological features of the *F*-region neutral wind field in the winter polar region and the location and spatial extent of the aurora. A definite correlation can be seen to exist between reversals and boundaries in the neutral wind field and the location of the visible auroral oval. Examples of such simultaneous data sets indicate that the neutral wind and boundaries closely follow the substorm-dependent expansion and contraction of the auroral oval.

2.1. Dependence of high-latitude thermospheric circulation on magnetospheric/ionospheric forcing processes

To study the dynamic response of the high-latitude thermosphere to various forcings in greater detail, data from many hundreds of DE 2 orbits, similar to those depicted in Figs 1 and 2, have been analysed. The FPI and WATS measurements of the two components of the upper thermospheric horizontal neutral wind vector, for example, have been binned and averaged according to various geophysical indices in order to investigate the mean response of the thermospheric neutral wind to forcings associated with the aurora. A primary conclusion is that above 60° of latitude the neutral wind pattern in the upper thermosphere is best ordered in a geomagnetic coordinate system (KILLEEN *et al.*, 1982; ROBLE *et al.*, 1983; HAYS *et al.*, 1984; REES *et al.*, 1985). The high-latitude neutral winds are observed generally to follow, but lag behind, the pattern of ionospheric convection, with some important differences. Thus, in Fig. 1, for example, the neutrals and ions have qualitatively similar velocities (speed and direction) throughout the high-latitude regions, with some important differences. In general, for example, the neutrals have a stronger sunward component in the dusk sector of

the auroral oval than in the dawn sector due to the differing effects of the Coriolis force for anticyclonic and cyclonic flow (KILLEEN and ROBLE, 1984).

MCCORMAC *et al.* (1987) used several hundred orbits of DE 2 over a six-month period to investigate quantitatively the dependence of the high-latitude thermospheric circulation on geomagnetic activity. Figure 4 shows the measured average neutral wind pattern using all available polar passes of DE 2 for active ($K_p > 4$) and quiet ($K_p \leq 3$) geomagnetic conditions in both hemispheres. The data are plotted in geomagnetic polar coordinates (magnetic local time and magnetic latitude). In all four cases, the mean neutral circulation shows the imprint of momentum transferred from the twin-cell ionospheric convection pattern, with strong anti-sunward winds over the geomagnetic polar cap bounded by strong sunward winds in the dusk auroral sector and much weaker sunward or anti-sunward winds in the dawn auroral sector. The magnitudes of the neutral winds are generally greater for the high K_p case than for the low K_p case, as would be expected from the stronger auroral forcings.

THAYER *et al.* (1987) further investigated the sensitivity of the high-latitude neutral circulation pattern to the sign of the east-west (B_y) component of the interplanetary magnetic field (IMF). They used average neutral wind measurements from the same data base as the MCCORMAC *et al.* (1987) study, discussed above, to illustrate changes in the configuration of the neutral wind pattern that were clearly ordered by the sign of B_y . Simultaneous measurements of B_y from the ISEE-3 spacecraft were used to select from and order the DE 2 neutral wind data. For this study, only data for which the north-south (B_z) component of the IMF was $\leq +1$ nT were used to avoid complications arising from the multi-cellular ion and neutral patterns known to exist for strongly northward IMF. Results from this study are shown in Fig. 5, in which data from ~ 300 orbits of DE 2 orbital passes have been separated according to the sign of B_y and averaged into bins of geomagnetic latitude and geomagnetic local time for the two hemispheres.

The criteria used to separate the data sets according to B_y involved the pre-existence of a definite positive or negative value for B_y , as measured by ISEE-3 for 1 h prior to the DE orbital pass. Passes occurring either during very high or very low levels of geomagnetic activity were excluded from the study and allowance was made for the propagation time to the Earth of the IMF measured at ISEE-3 altitudes. As can be seen from Fig. 5, there are significant differences in the mean thermospheric circulation patterns for B_y positive and negative. To some extent the effects are

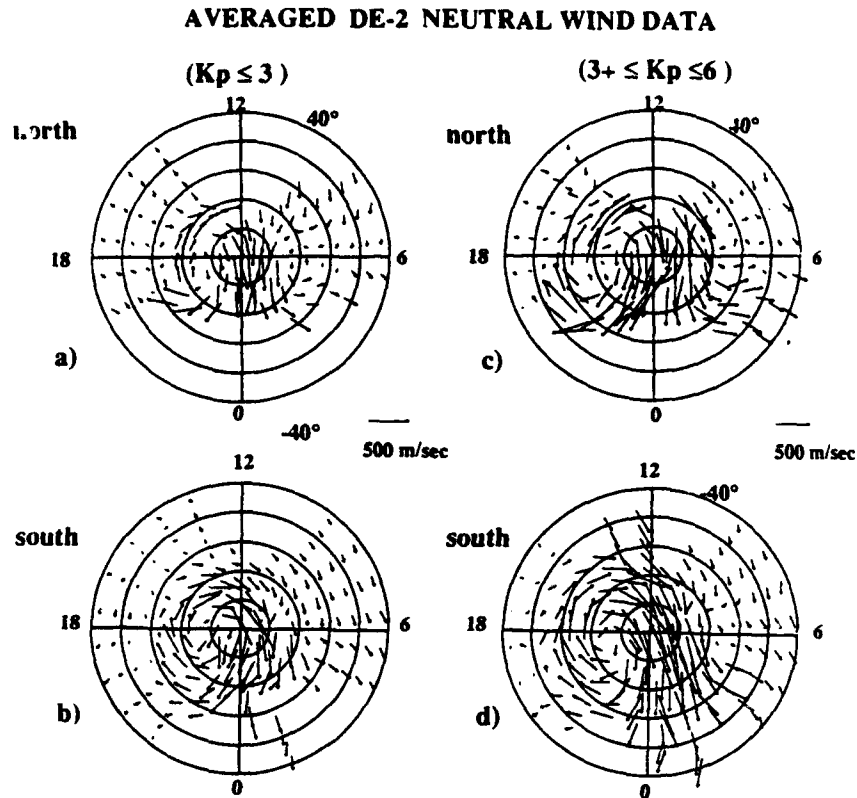


Fig. 4. Averaged upper thermospheric neutral wind measurements at ~ 300 km altitude for (a) north pole low K_p ; (b) south pole low K_p ; (c) north pole high K_p ; (d) south pole high K_p . Data collected between November 1981 and January 1982 and between November 1982 and January 1983 were averaged according to the given range of K_p and plotted in geomagnetic polar coordinates (magnetic latitude and magnetic local time). The outer circle of each polar dial is at 40° geomagnetic latitude.

mirrored between hemispheres; that is, a B_y positive (negative) signature in the northern hemisphere resembles a B_y negative (positive) signature in the southern hemisphere. In all cases, the average circulation patterns shown illustrate the dominance of the dusk anti-cyclonic neutral vortex mentioned above. The spatial magnitude of this vortex, however, is greater for B_y positive conditions in the northern hemisphere and for B_y negative conditions in the southern hemisphere. A distinct rotation in the direction of the polar cap anti-sunward flow that was dependent on the sign of B_y was also noted.

To highlight the structural changes in the neutral circulation pattern that are dependent on the sign of the B_y component of the IMF, Fig. 6 shows the average anti-sunward neutral wind (i.e. that component of the neutral wind parallel to the noon-midnight magnetic meridian) on the nightside of the geomagnetic polar cap as a function of magnetic local

time (MLT) for the magnetic latitude (MLAT) range $72.5-87.5^\circ$, where the data have been separated according to the sign of B_y for both hemispheres (THAYER, 1990). These plots illustrate more clearly the shift in location of the region of most rapid anti-sunward flow with a change in sign of B_y and demonstrate the 'mirroring' between hemispheres of this characteristic feature of the neutral circulation. In the northern hemisphere when B_y is positive (Fig. 6a), for example, the anti-sunward wind component reaches a maximum in the early morning sector at ~ 0400 MLT. When B_y is negative, the maximum in the anti-sunward wind component occurs in the pre-midnight sector at ~ 2200 MLT. These general results are reversed in the southern hemisphere, Fig. 6b. The locations of the various maxima in the anti-sunward polar-cap neutral wind are consistent with the locations of maxima in the B_y -dependent convection electric fields discussed by HEPNER (1977).

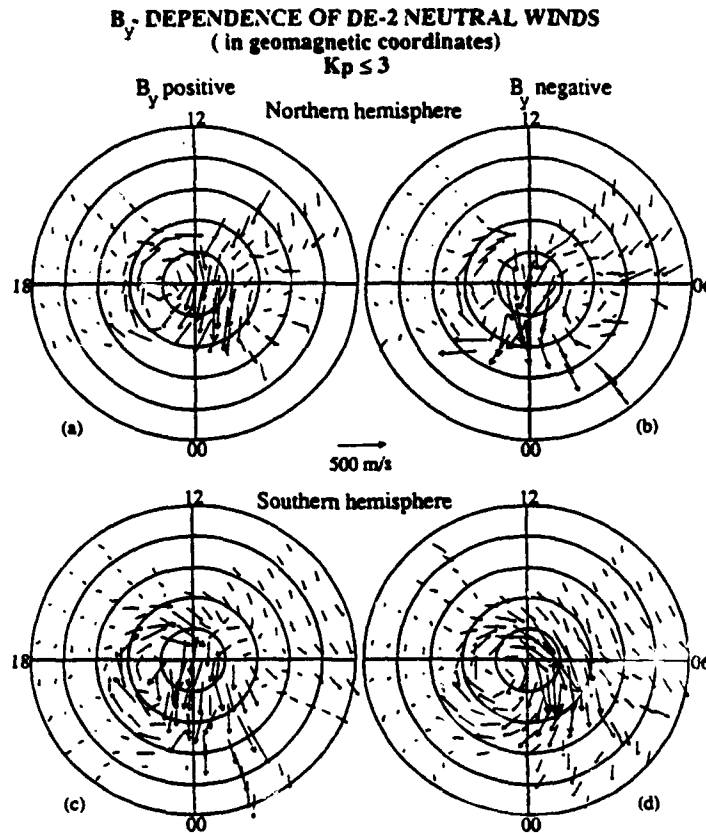


Fig. 5. Averaged upper thermospheric wind measurements for (a) north pole B_y positive; (b) north pole B_y negative; (c) south pole B_y positive; (d) south pole B_y negative. Data collected during the same period as for Fig. 4 were averaged according to the sign of the B_y component of the IMF and plotted in geomagnetic polar coordinates (magnetic latitude and local time). The outer circle of each polar dial is at 40 geomagnetic latitude.

The form of the neutral circulation for positive values of B_y at high latitudes has also been recently investigated. The existence of a region of sunward neutral wind flow in the central geomagnetic polar cap was noted by KILLEEN *et al.* (1985) for conditions of persistent large positive values of B_y . Two examples taken from this study are shown in Fig. 7. These two orbits (7210 and 7211) occurred during a prolonged period of strongly northward IMF ($B_z \sim 40$ nT) and both the ion drift measurements (red bars) and neutral winds (blue arrows) showed a region of sunward flow inside the geomagnetic polar cap. In a later study, MCCORMAC *et al.* (1991) systematically investigated the conditions for the occurrence of sunward polar cap neutral flow for northward B_z as a function of B_y using the entire DE 2 data base. They found that sunward winds generally only occurred when (i) B_y was persistently positive and (ii) the magnitude of B_y

was less than the magnitude of B_z . Figure 8, taken from the McCormac *et al.* study, is a scatter plot illustrating the IMF conditions for the occurrence of sunward (crosses) and anti-sunward (circles) neutral polar-cap flow. A total of 66 orbits were included in this study; in all cases the hourly averaged IMF B_z had been greater than 1 nT positive for the 4 h prior to the polar-cap orbital pass. It can be seen from this figure that sunward winds inside the polar cap rarely occur when the magnitude of the B_y component is greater than the magnitude of the corresponding B_z component (i.e. most occurrences of sunward flow [crosses] occur in the upper triangular section of the plot). This complex dependence of the neutral wind morphology on the relative magnitudes of individual IMF components is a phenomenon that clearly demonstrates the strong coupling among the magnetosphere, ionosphere and thermosphere.

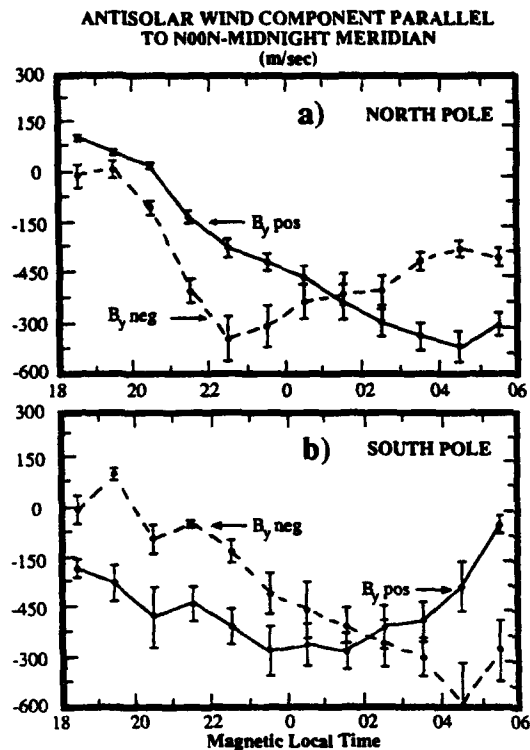


Fig. 6. Average anti-sunward neutral wind component parallel to the noon-midnight meridian in meters per second on the night side of the geomagnetic polar cap for both signs of B_z in the (a) northern and (b) southern hemispheres. The wind components have been averaged over magnetic latitudes between 72.5 and 87.5 and for each hour of magnetic local time from 1800 to 0600. The figure is taken from THAYER (1990).

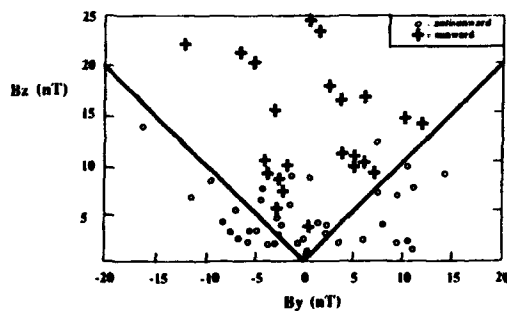


Fig. 8. Scatter plot of sunward and anti-sunward winds near the center of the geomagnetic polar cap as a function of the relative magnitudes of the B_x and B_y components of the interplanetary magnetic field. A total of 66 orbits are included in the plot. For all of the included orbits, the hourly averaged IMF B_z had been greater than 1 nT positive for the previous 4 h. This figure is taken from McCORMAC *et al.* (1991).

2.2. Vorticity and divergence in the high-latitude thermospheric wind pattern

The averaged measurements of thermospheric winds from DE 2 have enabled a study of the vorticity and divergence in the global-scale mean neutral flow in the high-latitude thermosphere to be conducted for the first time (THAYER and KILLEEN, 1991). In this work, data from two separate three-month intervals, centered on the winter solstices of 1981-1982 and 1982-1983, were averaged and binned according to geomagnetic latitude (MLAT) and local time (MLT). The DE 2 data were then analysed spectrally and merged with VSH model predictions as described by Thayer and Killeen to provide maps of the vorticity and divergence fields for (i) low geomagnetic activity and (ii) moderately high geomagnetic activity. These maps are shown in Fig. 9 for the northern hemisphere, winter case. Figure 9a and c shows the vorticity maps in geomagnetic polar coordinates for $K_p \leq 3$ conditions and $3+ \leq K_p \leq 6$ conditions, respectively, and Fig. 9b and d shows the divergence maps for the corresponding cases. These fields have been intentionally smoothed by the spectral truncation scheme used in manipulating the satellite data and they therefore represent the mean vorticity and divergence fields for the periods November 1981-January 1982, inclusive, and November 1982-January 1983, inclusive. Data from all Universal Times (UTs) were used to generate these maps, based on the assumption that the neutral wind field is largely invariant to UT when plotted in geomagnetic coordinates.

The derived vorticity patterns in units of inverse seconds, shown in Fig. 9a and c, describe the rotation in the flow field, where negative (positive) vorticity denotes anti-cyclonic (cyclonic) rotation. Since vorticity is generated by wind shear, the strong anti-sunward flow over the magnetic pole, combined with sunward flow in the dawn and dusk sectors, creates two regions of counter-rotating flow. Negative vorticity or anti-cyclonic rotation occurs primarily in the dusk sector, with a minimum value of $-518 \times 10^{-6} \text{ s}^{-1}$ for the low K_p case and $-596 \times 10^{-6} \text{ s}^{-1}$ for the high K_p case. Positive vorticity or cyclonic flow occurs primarily in the dawn sector with a maximum value of $426 \times 10^{-6} \text{ s}^{-1}$ for the low K_p case and $559 \times 10^{-6} \text{ s}^{-1}$ for the high K_p case. By comparing the vorticity fields for low and high K_p , it is evident that an enhancement in geomagnetic activity leads to enhanced vorticity in both dawn and dusk sectors and a general growth in the size of the region dominated by the twin vortices. The demarcation line of zero vorticity marks the region of shear reversals where the wind either reaches a maximum in the anti-

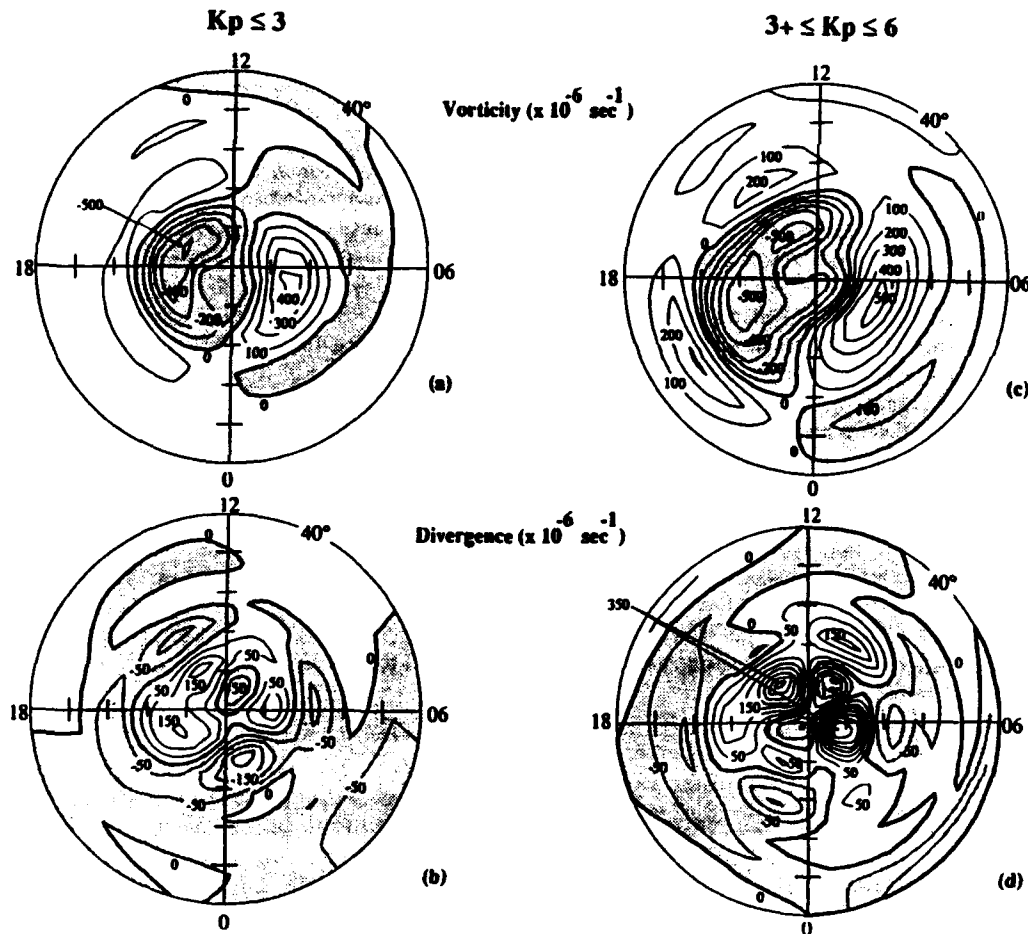


Fig. 9. Derived (a) vorticity pattern for the winter polar thermosphere at ~ 300 km altitude for conditions of low geomagnetic activity (northern hemisphere); (b) corresponding divergence pattern; (c) vorticity pattern for moderately active geomagnetic conditions; (d) corresponding divergence pattern. The patterns are shown in geomagnetic polar coordinates (magnetic latitude: pole to 40° and magnetic local time). The contour interval is $100 \times 10^{-6} \text{ s}^{-1}$ for the vorticity plots and $50 \times 10^{-6} \text{ s}^{-1}$ for the divergence plots. These plots were generated from spectrally analysed DE2 data and VSH model predictions (from THAYER and KILLEEN, 1991).

sunward direction in the central polar cap, or a maximum in the sunward direction in the dawn and dusk sectors. Thus, the transitions in the vorticity fields may be used to define the spatial dimensions of the high-latitude neutral circulation pattern. Below $\sim 60^\circ$ MLAT, the vorticity values are relatively small. The dominance of the signatures of the twin vortex motion induced in the high-latitude thermosphere by ion drag processes is evident in these maps which are strongly reminiscent of similar-looking maps of equipotentials for the polar electric fields (e.g. HEPPNER, 1977; HEELIS *et al.*, 1982).

The derived divergence patterns, shown in Fig. 9b and d, describe the rate of change of area in the flow fields determined by the longitudinal difference in the zonal wind components and the latitudinal difference in the meridional wind components, where negative values denote convergence in the flow field and positive values denote divergence. Once again, these fields represent mean patterns for the epoch in question and are plotted in units of inverse seconds. It can be seen that the divergence values are generally smaller (by about a factor of 4) than the vorticity values discussed above. This is due to the greater importance of the

largely divergence-free ion-drag momentum term in establishing the neutral circulation. Perturbations in the divergence fields are primarily forced by localized regions of heating, which can lead to upwelling and positive divergence, or regions of relative cooling, which can lead to downwelling or negative divergence (convergence). The divergence patterns are more complex than their vorticity counterparts and are characterized by localized islands of positive and negative divergence associated with regions of high-latitude heating and subsidence. The effect of enhanced levels of geomagnetic activity is to widen the area of large perturbations in the divergence fields and to intensify the maxima and minima observed. In these localized regions, the divergence field becomes commensurate with the vorticity field in magnitude.

The ability to generate thermospheric vorticity and divergence maps such as those shown in Fig. 9, provides a new tool for the interpretation of high-latitude thermospheric circulation patterns, allowing for a more detailed kinematic analysis of the flow configurations. In particular, this novel tool gives additional insight into the relative strengths of the various sources of momentum and energy responsible for driving the winds.

3. THE VECTOR SPHERICAL HARMONIC MODEL

The Vector Spherical Harmonic (VSH) model has been described by KILLEEN *et al.* (1987). It is a semi-empirical 'hybrid' model that is based on numerical simulations of the NCAR-TIGCM and available experimental data from DE2. The NCAR-TIGCM solves the primitive equations of dynamic meteorology adapted to thermospheric altitudes, including equations for the conservation of energy and momentum and the individual species continuity equations. The physics inherent in the model's parameterizations and input prescriptions are those appropriate to thermospheric altitudes. The basic model and subsequent major developments have been described in detail by DICKINSON *et al.* (1981, 1984), ROBLE *et al.* (1982), FESEN *et al.* (1986) and ROBLE and RIDLEY (1987). Most recently, the model was further extended (ROBLE *et al.*, 1988) to include a self-consistent aeronomic scheme for the thermosphere and ionosphere using a fully Eulerian approach.

The VSH model uses output from various 'generic' runs of the TIGCM to develop a library of truncated spectral coefficients that represent the global thermospheric wind, temperature and neutral composition fields for a set of different geophysical conditions (solar maximum, solar minimum, equinox,

solstice, etc.). The three-dimensional wind field is represented by a vector spherical harmonic expansion in the horizontal, a Fourier expansion in Universal Time and a polynomial expansion in altitude. The global temperature field differs in that a scalar spherical harmonic expansion is used in the horizontal and a Bates model profile is used in the vertical. Neutral composition fields are described using logarithmic scalar harmonic expansions. The thermospheric state variables (wind, temperature and composition) may then be calculated simply using a computer subroutine which reads in the coefficients and regenerates the required field as a function of space and time and geophysical condition ($F10.7$ value and A_p). Recently, data from DE2 have also been incorporated into the VSH model description using an objective analysis scheme to merge the experimental data and theoretically calculated TIGCM gridded output fields. In this objective analysis scheme, measurements from DE2 are used whenever available, and TIGCM model results are used in the absence of experimental data, with the whole process being carried out in the spectral domain to provide for smooth merger of the experimental and theoretical results.

3.1. VSH model comparisons with thermospheric wind observations

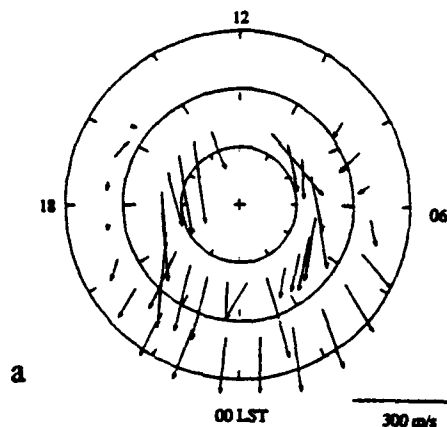
An example of a comparison between the global output of the VSH model and averaged DE2 data is shown in Fig. 10. The lower part of this figure (10b) shows the bin-averaged neutral wind field from FPI and WATS as a function of UT and latitude, coded as vectors, for the same two three-month study periods as for the previous results shown earlier. The thermospheric temperatures from FPI and WATS are coded as colors according to the scale at the right. As can be seen, the largest wind speeds are observed in the two high-latitude regions (southern hemisphere polar regions towards the lower part of the plot and northern hemisphere polar regions towards the upper part). The measured thermal structure indicates a relatively hot summer polar region (temperatures up to ~ 1500 K) and a relatively cold low-latitude region (blue band in middle of plot—temperatures ~ 900 K). For comparison, Fig. 10a shows the equivalent output from the VSH model, where the model was interrogated to provide calculated December solstice wind and temperature fields in the same format as the experimental data. As can be seen, there is reasonable agreement between the model and the global-scale experimental data. The seasonal thermal structure (summer-to-winter gradient) is present in the model which, however, tends to underestimate the northern polar

temperatures. The wind pattern shows reasonable agreement also, though there is considerably more structure in the experimental results than in the model predictions. The morphology of the high-latitude flows and reversals are generally well matched by the model.

To provide additional comparisons with the new VSH model, Figs 11 and 12 show comparisons with ground-based thermospheric neutral wind measurements. Fig. 11a shows thermospheric wind measurements from two optical observatories in Greenland, one at Thule (76.0° N, 70.0° W) in the central region of the geomagnetic polar cap and one at Sondrestrom (67.0° N, 51.0° W) on the northern edge of the auroral zone. The winds shown represent bin-averaged data for geomagnetic quiet times ($K_p \leq 3$), taken during the 1987-1988 observing season (September-March). The vectors shown represent bin-averaged winds at ~250 km altitude from both stations for all available clear nights of observations during low geomagnetic activity conditions ($K_p \leq 3$), plotted in polar geographic coordinates. The inner set of vectors show the averaged winds from Thule and the outer set of vectors show the winds from Sondrestrom. For comparison, Figure 11b shows the output from the VSH model which was interrogated to match the conditions appropriate to the experimental results. The measured winds show a largely anti-sunward flow over the polar cap, bounded on the dusk side with a region of sunward flow, and with a turning and abatement of the winds on the dawn side of the polar cap. The comparison between experiment and model indicates reasonable agreement, with the major characteristics of the flow pattern being well represented by the model. There are some discrepancies, however, notably in the direction of the strong anti-sunward flow over Sondrestrom near midnight.

Figure 12 shows experimental neutral wind data from the incoherent scatter radar at Sondrestrom, separated according to the sign of the IMF B_z component. These data represent approximately 2200 h of measurements obtained between April 1983 and July 1988. The radar winds are averaged between 210 and 360 km altitude. The VSH model was interrogated to provide predictions for the neutral winds during these periods and these results are shown in Fig. 12. The agreement between the VSH model predictions and the radar-determined winds for the given site is again reasonable, perhaps with the exception of the early morning period for B_z positive where the model overestimates the magnitude of the measured wind. Since the empirical component of the VSH model is provided by DE2 measurements referred to the 1981-1983 solar maximum period, it is encouraging to note

Thule and Sondre Stromford FPI - $K_p \leq 3$, 1987/8



Thule and Sondre Stromford - VSH winds, solar min., low K_p

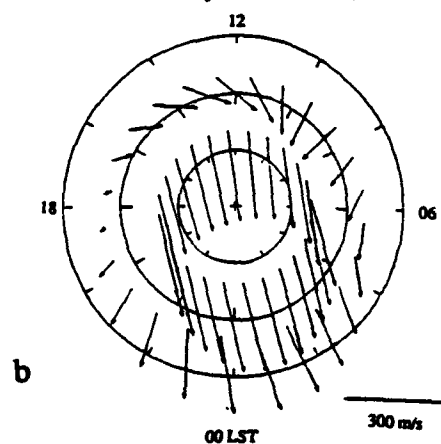


Fig. 11. (a) Measured neutral winds at ~250 km altitude determined from the Fabry-Perot observatories at Thule and Sondrestrom, Greenland, during the observing season of 1987-1988. The data represent bin-averaged winds for all clear-sky observations from the two stations. The winds are coded as arrows (scale at lower right) with the base of the arrow located at the appropriate local time and latitude for the particular station. The Thule measurements constitute the inner circle of vectors and the Sondrestrom measurements constitute the outer circle of vectors. (b) VSH model predictions for the corresponding geophysical conditions.

the degree of model agreement with neutral wind data obtained from a quite different time period and phase of the solar cycle.

4. THERMOSPHERIC COMPOSITION PERTURBATIONS AT HIGH LATITUDES

The results described above have demonstrated various characteristics of the mean thermospheric

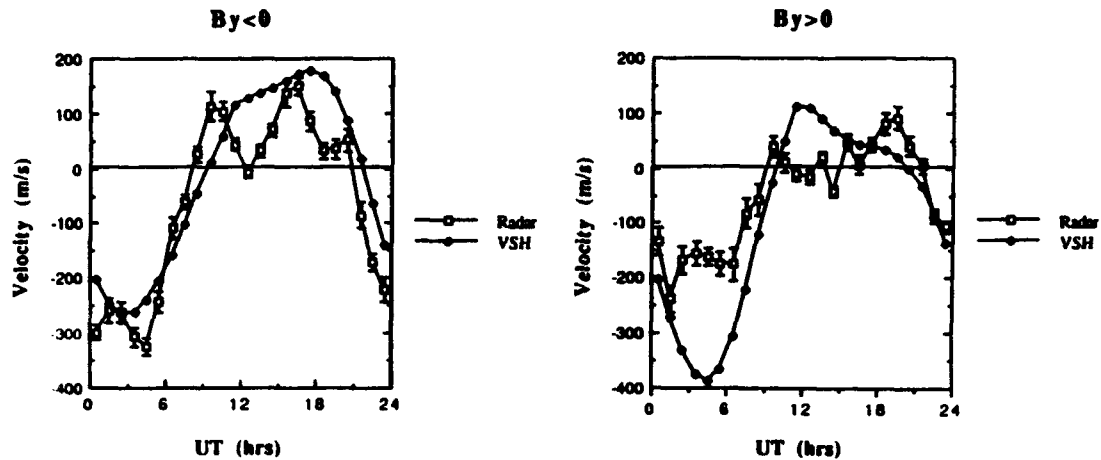


Fig. 12. Comparison of Sondrestrom incoherent scatter radar average meridional winds (in the magnetic meridian) with predictions of the Vector Spherical Harmonic Model (KILLEEN *et al.*, 1987) as a function of IMF B_z orientation for B_z negative conditions. The radar data set includes approximately 2200 h of measurements obtained from April 1983 to July 1988. Radar winds were first averaged over hourly intervals from 210 to 360 km for each experiment. The average winds as a function of UT and IMF orientation were then determined by binning the entire data set as a function of UT hour and average IMF orientation during the period from 1 to 2 h prior to the beginning of each hourly bin. The figure is taken from JOHNSON *et al.* (1991).

neutral circulation at high geomagnetic latitudes. The wind patterns show a circulation that has a strong rotational component associated with the twin-cell ionospheric convection pattern, with a significant divergent component driven largely by pressure gradient forcing. It might be expected that the large magnitude horizontal neutral winds and associated vertical motions would have a significant effect on the compositional balance of the upper thermosphere. To investigate this possibility, BURNS *et al.* (1989) have used the NCAR-TIGCM to study the changes in thermospheric composition that result from wind systems such as discussed above. Figure 13 shows an example of a set of calculations from their work, illustrating the various dynamical forcing terms for thermospheric composition variations during and in the aftermath of a simulated geomagnetic storm.

This figure shows NCAR-TIGCM calculations of the terms responsible for changes in the mass mixing ratio of N_2 (Ψ_{N_2}) during the large geomagnetic storm that occurred on 24 November 1982. The terms are referred to an altitude of ~ 280 km and the location of the geomagnetic pole is shown as the cross in Fig. 13d. The plots show the differences between storm and quiet times for the following terms: (a) vertical advective forcing of Ψ_{N_2} ; (b) horizontal advective forcing of Ψ_{N_2} ; (c) molecular diffusion effects and (d) Ψ_{N_2} itself. The first three plots (13a–c), showing com-

positional adjustment forcing terms, are for 14 UT, some 3 h after the commencement of the storm, and the plot showing the mass mixing ratio (13d) is for 19 UT or 2 h into the storm simulation. Thus, these plots illustrate some of the physical forcing processes that give rise to the changes in mass mixing ratio at ~ 280 km a few hours after the commencement of a large geomagnetic storm.

The pattern of compositional forcing that is seen at high latitudes for this storm-time case results from both horizontal and vertical advection, where the horizontal and vertical winds are due primarily to ion drag and Joule heating, respectively. Figure 13a illustrates the rate of change of mass mixing ratio due to the advective effects of vertical winds. A region of positive values (associated with upwelling near regions of enhanced heating) can be seen to be roughly coincident with the location of the auroral zone and regions of negative forcing (associated with subsidence) can be seen to lie equatorward of the auroral zone and within the geomagnetic polar cap. Figure 13b illustrates the rate of change of Ψ_{N_2} due to the advective effects of horizontal winds. The region of large positive values in the post-midnight sub-auroral sector is due to the existence of the post-midnight surge in the meridional winds which tends to increase the mass mixing ratio of nitrogen downstream from the polar regions. Figure 13c illustrates the rate of change

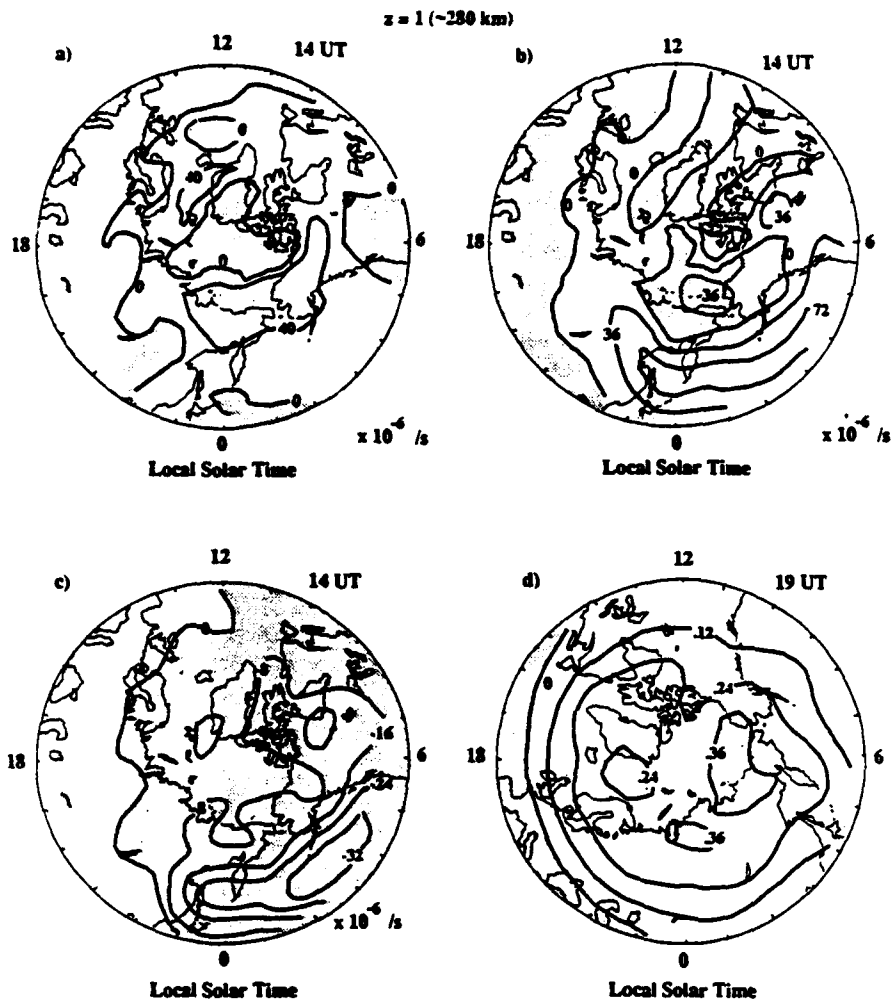


Fig. 13. NCAR-TIGCM calculations of the forcing terms responsible for changes in the mass mixing ratio of N_2 (Ψ_{N_2}) during the large geomagnetic storm that occurred on 24 November 1982. The plots show the mass-mixing-ratio forcing-term differences between storm and quiet times for the following: (a) vertical advection; (b) horizontal advection; (c) molecular diffusion and (d) (Ψ_{N_2}). The first three terms are for 14 UT, some 3 h after the commencement of the storm, and the last plot, showing mass mixing ratio, is for 19 UT. The cross in Fig. 13d indicates the location of the geomagnetic pole.

of Ψ_{N_2} due to molecular diffusion. This term tends to be negative throughout the high-latitude region as it attempts to restore the thermosphere to the diffusive equilibrium that has been interrupted by the high-latitude dynamical processes. Maximum values of the perturbed Ψ_{N_2} (Fig. 13d) are found in the auroral and sub-auroral morning sector, in agreement with the DE 2 observations reported by HEDIN and CARRIGAN (1985). The magnitudes of the three terms shown in

Fig. 13a-c are roughly commensurate, indicating that all three processes (vertical and horizontal advection and molecular diffusion) are of roughly equal importance in the establishment of the storm-time compositional state of the high-latitude thermosphere. This type of quantitative compositional forcing term analysis thus enables a deeper insight into the coupling of dynamics and composition in the high-latitude thermosphere.

5. CONCLUDING REMARKS

Recent experimental results from the Dynamics Explorer-2 spacecraft and ground-based optical and radar observatories have illustrated the manner by which the high-latitude processes of ion drag and Joule heating control the behavior of the high-latitude upper thermosphere. The neutral winds at high altitudes typically tend to follow the twin-cell pattern of ionospheric convection, as momentum is transferred from the ions to the neutrals at a rate that is proportional to the ion density. As a consequence of this tight ion-neutral momentum coupling, the neutral wind pattern displays strong dependencies on the level of geomagnetic activity and on the orientation of the interplanetary magnetic field, much in the same way as the ionospheric convection pattern does itself. Neutral wind vortices are established whose geometries and intensities depend on the nature and time-history of the momentum forcing. Upper thermospheric temperatures are directly controlled by the Joule and particle heat sources associated with auroral latitudes. The auroral heating also serves to modulate the thermospheric circulation through the generation of

strong pressure-gradient forces and through local upwelling of the atmosphere. Changes in the vertical and horizontal winds at high latitudes lead, in turn, to neutral compositional perturbations. The various dynamical, energetic and compositional variations associated with auroral processes are thus highly coupled with each other.

Significant progress has been made recently in the development of semi-empirical models of the thermosphere that utilize the large and comprehensive new data resources. One of these models, the Vector Spherical Harmonic model, has been shown to provide reasonably accurate predictions for global-scale thermospheric wind systems.

Acknowledgements—This work was supported by the NASA grant NAG5-465 and by NSF grants ATM-8918476, ATM-8822530, ATM 9096134 and ATM 9002608 and by Geophysics Laboratory grant F19628-89-K-0047 to the University of Michigan. Dynamics Explorer science team members who kindly provided data for this work include Drs R. A. Heelis, W. B. Hanson, L. A. Frank, J. D. Craven, L. H. Brace, W. R. Hoegy, N. W. Spencer and G. R. Carignan. We also thank Dr R. G. Roble for numerous discussions and for providing TIGCM model results.

REFERENCES

- | | | |
|---|------|--|
| BURNS A. G., KILLEEN T. L. and ROBLE R. G. | 1989 | <i>J. geophys. Res.</i> 94 , 3670. |
| CARIGNAN G. R., BLOCK B. P., MAURER J. C.,
HEDIN A. E., REBER C. A. and SPENCER N. W. | 1981 | <i>Space Sci. Instrum.</i> 5 , 493. |
| DICKINSON R. E., RIDLEY E. C. and ROBLE R. G. | 1981 | <i>J. geophys. Res.</i> 86 , 1499. |
| DICKINSON R. E., RIDLEY E. C. and ROBLE R. G. | 1984 | <i>J. atmos. Sci.</i> 41 , 205. |
| FESEN C. S., DICKINSON R. E. and ROBLE R. G. | 1986 | <i>J. geophys. Res.</i> 91 , 4471. |
| FRANK L. A., CRAVEN J. D., ACKERSON K. L.,
ENGLISH M. R., EATHER R. H. and
CAROVILLANO R. L. | 1981 | <i>Space Sci. Instrum.</i> 5 , 369. |
| FULLER-ROWELL T. J., QUEGAN S., REES D.,
MOFFETT R. J. and BAILEY G. J. | 1987 | <i>J. geophys. Res.</i> 92 , 7744. |
| FULLER-ROWELL T. J. and REES D. | 1980 | <i>J. atmos. Sci.</i> 37 , 2545. |
| HANSON W. B., HEELIS R. A., POWER R. A.,
LIPPINCOTT C. R., ZUCCARO D. R., HOLT B. J.,
HARMON L. H. and SANATANI S. | 1981 | <i>Space Sci. Instrum.</i> 5 , 395. |
| HAYS P. B., KILLEEN T. L. and KENNEDY B. C. | 1984 | <i>J. geophys. Res.</i> 89 , 5597. |
| HAYS P. B., KILLEEN T. L., SPENCER N. W.,
WHARTON L. E., ROBLE R. G., EMERY B. A.,
FULLER-ROWELL T. J., REES D., FRANK L. A.
and CRAVEN J. D. | 1991 | <i>J. geophys. Res.</i> 96 , 7657. |
| HEDIN A. E., BIONDI M. A., HERNANDEZ G.,
BURNSIDE R. G., JOHNSON R. M., KILLEEN T. L.,
MAZAUDIER C., MERIWETHER J. W., SALAH J. E.,
SICA R. J., SMITH R. W., SPENCER N. W.,
WICKWAR V. B. and VIRDI T. S. | 1985 | <i>J. geophys. Res.</i> 90 , 5269. |
| HEDIN A. E. and CARIGNAN G. R. | 1988 | <i>J. geophys. Res.</i> 93 , 9959. |
| HEDIN A. E., SPENCER N. W. and KILLEEN T. L. | 1981 | <i>Space Sci. Instrum.</i> 5 , 511. |
| HEELIS R. A., HANSON W. B., LIPPINCOTT C. R.,
ZUCCARO D. R., HARMON L. H., HOLT B. J.,
DOHERTY J. E. and POWER R. A. | 1982 | <i>J. geophys. Res.</i> 87 , 6339. |
| HEELIS R. A., LOWELL J. K. and SPIRO R. W. | 1977 | <i>J. geophys. Res.</i> 82 , 1115. |
| HEPPNER J. P. | | |

- JOHNSON R. M., DE LA BEAUJARDIERE O.
and KILLEEN T. L. 1991 *J. geophys. Res.* (unpublished manuscript).
- KILLEEN T. L. 1987 *Rev. Geophys.* **25**, 433.
- KILLEEN T. L., CRAVEN J. D., FRANK L. A.,
PONTHIEU J.-J., SPENCER N. W., HEELIS R. A.,
BRACE L. H., ROBLE R. G., HAYS P. B.
and CARIGNAN G. R. 1988 *J. geophys. Res.* **93**, 2675.
- KILLEEN T. L., HAYS P. B., SPENCER N. W.
and WHARTON L. E. 1982 *Geophys. Res. Lett.* **9**, 957.
- KILLEEN T. L., HEELIS R. A., HAYS P. B.,
SPENCER N. W. and HANSON W. B. 1985 *Geophys. Res. Lett.* **12**, 159.
- KILLEEN T. L. and ROBLE R. G. 1984 *J. geophys. Res.* **89**, 7509.
- KILLEEN T. L. and ROBLE R. G. 1988 *Rev. Geophys.* **26**, 329.
- KILLEEN T. L., ROBLE R. G.
and SPENCER N. W. 1987 *Adv. Space Res.* **7**, 207.
- KREHBIEL J. P., BRACE L. H., THEIS R. F.,
PINKUS W. H. and KAPLAN R. B. 1981 *Space Sci. Instrum.* **5**, 493.
- MAYR H. G., HARRIS I., VAKOSI F.,
HERRERO F. A., VOLLAND H., SPENCER N. W.,
HEDIN A. E., HARTLE R. E., TAYLOR H. A. JR.,
WHARTON L. E. and CARIGNAN G. R. 1985 *Adv. Space Res.* **5**, 283.
- MCCORMAC F. G., KILLEEN T. L.
and THAYER J. P. 1991 *J. geophys. Res.* **96**, 115.
- MCCORMAC F. G., KILLEEN T. L., THAYER J. P.,
TSCHAN C. R., HERNANDEZ G., PONTHIEU J.-J.
and SPENCER N. W. 1987 *J. geophys. Res.* **92**, 10133.
- MERIWETHER J. W. JR 1983 *Radio Sci.* **18**, 1035.
- REES D., GORDON R., FULLER-ROWELL T. J.,
SMITH M., CARIGNAN G. R., KILLEEN T. L.,
HAYS P. B. and SPENCER N. W. 1985 *Planet. Space Sci.* **33**, 617.
- ROBLE R. G. 1983 *Rev. Geophys. Space Phys.* **21**, 217.
- ROBLE R. G., DICKINSON R. E.
and RIDLEY E. C. 1982 *J. geophys. Res.* **87**, 1599.
- ROBLE R. G., DICKINSON R. E., RIDLEY E. C.,
EMERY B. A., HAYS P. B., KILLEEN T. L.
and SPENCER N. W. 1983 *Planet. Space Sci.* **31**, 1479.
- ROBLE R. G. and RIDLEY E. C. 1987 *Ann. Geophys.* **5A**, 369.
- ROBLE R. G., RIDLEY E. C., RICHMOND A. D.
and DICKINSON R. E. 1988 *Geophys. Res. Lett.* **15**, 1325.
- SPENCER N. W., WHARTON L. E., NIEMANN H. B.,
HEDIN A. E., CARIGNAN G. R.
and MAUREN J. C. 1981 *Space Sci. Instrum.* **5**, 417.
- THAYER J. P. and KILLEEN T. L. 1991 *J. geophys. Res.* (unpublished manuscript).
- THAYER J. P., KILLEEN T. L.,
MCCORMAC F. G., TSCHAN C. R.,
PONTHIEU J.-J. and SPENCER N. W. 1987 *Ann. Geophys.* **5A**, 363.
- Reference is also made to the following unpublished material:*
- THAYER J. P. 1990 Ph.D. thesis, University of Michigan, Ann Arbor, MI 48109, U.S.A.

THE BEHAVIOR OF THE HIGH-LATITUDE F-REGION NEUTRAL THERMOSPHERE IN RELATION TO IMF PARAMETERS

R. J. Niciejewski,* T. L. Killeen,* R. M. Johnson* and
J. P. Thayer**

* *Space Physics Research Laboratory, Department of Atmospheric, Oceanic
and Space Sciences, The University of Michigan, Ann Arbor, MI 48109, U.S.A.*

** *Geosciences and Engineering Center, SRI International, Menlo Park,
CA 94025, U.S.A.*

ABSTRACT

Ground based incoherent scatter radar (ISR) and Fabry Perot interferometer (FPI) studies in the northern high latitudes during the period 1983 to 1989 have shown that the F-region neutral wind field pattern depends upon the sign of the IMF parameters. For example, the cell structure of the northern hemisphere high latitude neutral wind field during periods of low geomagnetic activity depends to a large degree upon the sign of the IMF B_y parameter.

Long term monitoring of the F-region thermosphere by FPI in Thule, Greenland, and by both FPI and ISR in Søndre Strømfjord, Greenland, have made it possible to produce maps of average meridional and zonal wind fields for various IMF configurations for northern high latitudes. Comparison of observations with theoretical wind field modelling, such as the Vector Spherical Harmonic model, indicates that most observed features are consistent with the models.

INTRODUCTION

Neutral winds in the polar cap F-region are controlled by a combination of pressure gradient forces and ion drag forces, the latter being the primary driving force at high latitudes. Coupling between the ion and the neutral constituents in the F-region thermosphere, which is dependant upon the ion neutral collision frequency, forces the neutral component to follow the ion drift convection pattern with an appropriate time constant. As a result, the F-region neutral wind circulation pattern for high latitudes usually exhibits a similarity to the ion convection cell pattern.

The configuration of the Interplanetary Magnetic Field (IMF) has a marked effect upon the size and geometry of the ion convection cell pattern, and consequently, the neutral circulation pattern. In particular, the sign of the B_y component of the IMF controls the relative size of the dawn and dusk ionospheric circulation cells. However, the time constant for momentum transfer from ions to neutrals is of the order of several hours, implying that rapid changes in the IMF are not immediately apparent in the neutral wind pattern. Several studies have been published which document the influence of the B_y component on the high latitude thermosphere: ground-based optical /1-5/, ground-based radar /6/, satellite /7/, and theoretical studies /8/.

In this study, data acquired by optical techniques at Søndre Strømfjord and Thule, Greenland are used to construct averaged horizontal winds for both signs of the IMF B_y component. These results are compared with predicted thermospheric circulation patterns from a Vector Spherical Harmonic (VSH) model. The comparison indicates that this model provides a reasonable representation of the optically observed horizontal wind components in the thermosphere for the two signs of the IMF B_y component. Finally, the averaged neutral winds derived from the incoherent scatter radar at Søndre Strømfjord for the same geomagnetic conditions are compared with the optical measurements and the modelled winds.

RESULTS

Similar Fabry Perot interferometers are located in both Søndre Strømfjord and Thule, Greenland, the

former collocated with an incoherent scatter radar system. The optical instrument is described in *Meriwether et al.* [4]. The interferometers were in routine, automated operation during the solar minimum period acquiring F-region neutral wind measurements during dark sky periods through the entire optical observing season - September to April. Cloud cover data for both stations was obtained from the Danish Meteorological Institute and the United States Air Force for Søndre Strømfjord and Thule, respectively. This information permitted the removal of data acquired during non-ideal observing periods. Geomagnetic indices and IMF values (in Geocentric Solar Magnetospheric coordinates) were obtained from the NSSDC data base. In total, four years of Søndre Strømfjord data and three years of Thule data during solar minimum were used to generate the final averages. The horizontal wind components may be considered as representative of the neutral wind pattern for the northern polar cap for conditions of average geomagnetic activity during the solar minimum period.

The conditions chosen for the binning process are similar to those used by *Thayer et al.* [7]. The IMF parameters used in the current sorting scheme were one hour averages for both B_y and B_z , which is the same resolution as the cloud cover data. Each horizontal wind measurement was assigned B_y , B_z , K_p , and cloud index values. The winds were then sorted into one hour wide bins based upon the following criteria: a) low geomagnetic activity ($K_p \leq 3$); b) southward B_z component ($B_z < 1$ nT); c) the sign of B_y constant for at least two hours preceding the wind measurement; d) no inclusion of wind data within the bins if there are no IMF data available for the measurement period; e) cloud cover must be low. This strict filtering criteria reduced the neutral wind data set to slightly over 2% of its original size.

Figures 1a) and 1b) display the results of the sorting analysis. The figures are shown using a geomagnetic latitude/magnetic local time coordinate system in a polar dial display. The length of the vector is proportional to the magnitude of the horizontal wind as indicated by the vector in the bottom right-hand corner. The tail of a vector is located at the geomagnetic latitude of the station and the magnetic hour of the bin. The outer ring of vectors corresponds to F-region neutral winds over Søndre Strømfjord, while the inner ring shows the same for Thule. Even though Søndre Strømfjord is at the arctic circle, there are still periods at winter solstice during which the sky illumination is too high to perform data acquisition. As a result, this ring of data does not cover an entire day. Figure 1a) refers to B_y negative conditions, while Figure 1b) shows B_y positive results.

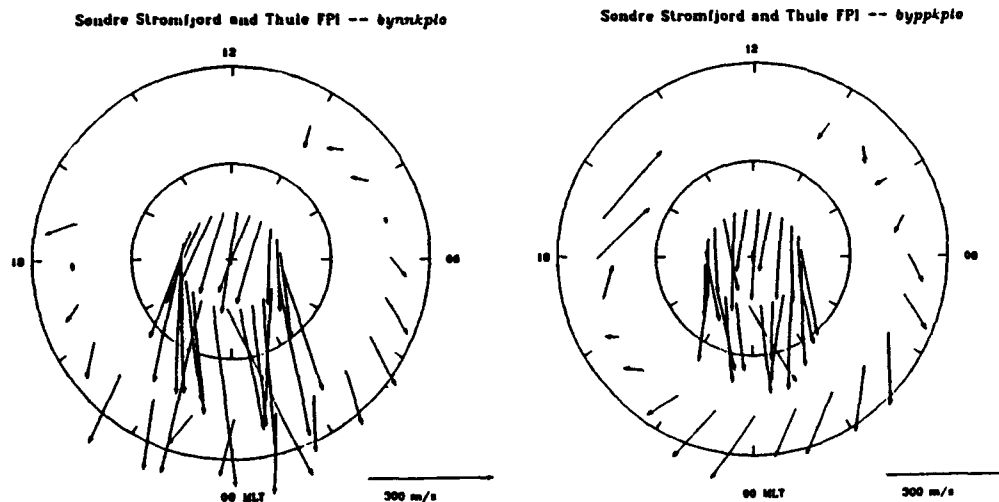


Fig. 1. a) Polar dial plot representing average horizontal neutral wind vectors in the F-region thermosphere. The coordinate system is geomagnetic latitude/corrected geomagnetic local time. The plot is centered on the north geomagnetic pole with circles shown for 80° and 70° latitude. The magnitude of the horizontal neutral wind is proportional to the length of the vector, as shown by the arrow in the lower right corner. The location of the tails of the vectors correspond to the geomagnetic latitudes of Thule (inner circle) and Søndre Strømfjord (outer circle). This panel is for B_y negative conditions, filtered as described in the text. b) Same as a) but for B_y positive conditions.

The neutral wind model chosen for the comparison was the VSH model [9]. This is a computer model which provides time dependent, horizontal neutral wind vectors. This model consists of a set of coefficients derived from geophysical field outputs generated by a selection of various NCAR thermospheric general circulation model runs. A vector spherical harmonic expansion of the coefficients is used to represent the wind field, while a Fourier expansion represents the temporal dimension.

In this study, two diurnally reproducible NCAR TGCM "steady state" runs were chosen for comparison with the optically measured winds, one for the B_y positive case and the other for the B_y negative case. Both runs were made for conditions of average geomagnetic during the solstice periods. Average geomagnetic activity was defined as: a) $K_p = 3$; b) $A_p = 20$; c) cross-cap potential = 30 kV. In both runs, the absolute magnitude of B_y was 7 nT.

Neutral winds derived from incoherent scatter radar data for Søndre Strømfjord have previously been presented for similar conditions by *de la Beaujardière and Wickwar [6]*. In their study, neutral winds from a two year set were used. In the current study, neutral winds derived from the entire radar data base (April, 1983 to July, 1988) were used to construct averaged neutral winds in the geomagnetic meridional direction. Prior to sorting of the winds according to IMF conditions, the winds for range gates between 210 and 360 km were averaged to generate a single value representing the neutral thermospheric meridional wind in the F-region. Next, the winds were sorted into one hour wide bins using similar B_y and B_z criteria as for the optical data sorting, the only difference being that the hourly averaged wind measurements were associated with the average of the IMF parameters obtained 1 to 2 hours prior to the wind measurements.

A comparison of the observed neutral winds with the modelled neutral winds is shown in Figures 2a) and 2b), the former for B_y negative conditions and the latter for B_y positive conditions. Here, only the averaged geomagnetic meridional winds as a function of time for Søndre Strømfjord are shown. The statistical uncertainty in the mean is also indicated for both the radar (R) and optical (O) averages. There are no optical measurements between 13 and 18 hours Universal Time since this period brackets local noon in Søndre Strømfjord.

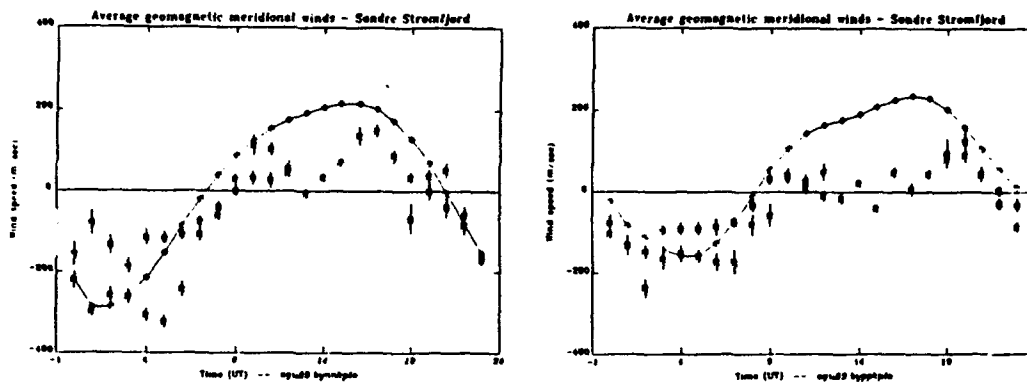


Fig. 2. a) Average neutral meridional winds for Søndre Strømfjord, Greenland in the geomagnetic meridian. The average neutral winds acquired experimentally are shown with their respective statistical uncertainties in their means: O refers to FPI data and R refers to ISR data. The curve displays the corresponding model winds from the VSH code. This panel refers to B_y negative conditions. b) Same as a) but for B_y positive conditions.

DISCUSSION

Several features are obvious from the polar dial plots of Figure 1 and the collated data in Figure 2. For B_y positive conditions, the magnitude of the horizontal neutral winds is smaller in Thule than for B_y negative periods. In addition, the magnitude of the meridional winds measured at Søndre Strømfjord is smaller for B_y positive. Although not shown here, the absolute magnitude of the experimental averaged zonal winds for Søndre Strømfjord is larger for the B_y positive case, unlike the meridional averages. Assuming a two cell structure in the neutral horizontal wind flow within the polar cap and fitting that with the observed horizontal wind vectors indicates that during the B_y negative case the cells appear to be similar in size. Likewise, for the B_y positive condition, an asymmetry is apparent between the two cells, the dusk cell being much larger in size than the dawn cell, encroaching into the dawn sector.

The behavior of the presumed cell structure of the neutral wind field as a function of the sign of IMF B_y within this study has some similarities with the comprehensive study performed by *Thayer et al. [7]*. Their work is based upon DE2 satellite measurements of the neutral wind field during solar maximum. The asymmetry in the cell pattern during B_y positive in the northern hemisphere observed by the satellite is also evident during the current study's solar minimum observations. They also observed a symmetric pattern during B_y negative conditions. However, the large surge that they observed in the magnitude of the winds at $\sim 75^\circ$ invariant latitude during B_y positive periods is not evident during the solar minimum study. Similarities between the averaged wind vectors in Figure 1a) and 1b) and the data presented by *Meriwether and Shih [3]*, for Søndre Strømfjord and *Meriwether et al. [4]*, for Thule are also evident. In the latter two studies, individual nights of data were shown to display a B_y dependence: an enlargement in the evening cell towards the morning cell for B_y positive conditions.

The observed geomagnetic meridional neutral winds shown in Figures 2a) and 2b) show reasonable agreement with the VSH model winds during dark conditions. In both the B_y negative and the B_y positive cases, the phase of the observed wind is similar to the modelled wind with zero crossings differing by no more than about one hour. The magnitude of the observed winds during dark hours is similar to the modelled winds, but both the optical and the radar winds show structure in the binned averages. The fact that the optical winds differ from the radar neutral winds is not surprising since there were very few, if any, coordinated measurements between the two sets of observations. The greatest discrepancy between the model and the observations occurs during daylight conditions. This also is not too surprising when consideration is made regarding the geometry of the auroral oval with respect to Søndre Strømfjord. The cusp/cleft region passes through the geomagnetic meridian over this station at approximately 1400 UT which corresponds to the period of greatest discrepancy. The modelled results provide wind vectors on a 5° by 5° grid which tends to average the fine structure expected in the cusp/cleft area. In addition, the observations correspond to a range of K_p indices, while the modelled results are calculated for $K_p = 3$. Søndre Strømfjord is at the location of the dayside boundary between the polar cap and the sub auroral region, and as a result, neutral wind measurements acquired during midday periods will be very sensitive to the latitude of the cusp/cleft. It is not clear from this data set the cause of the discrepancy between the midday winds and the model, but it seems likely that the differences are due to sampling winds in or about the cleft.

In summary, we have sorted several years of optical and radar data based upon the sign of the IMF B_y component. In all cases, the IMF B_z component was taken to be near zero, or definitely southward. The binned averages from the optical measurements in Thule and Søndre Strømfjord have been displayed in a polar dial form for both signs of B_y and indicate a definite asymmetry in the cell size of the neutral wind convection pattern for B_y positive conditions. The cells appear to be similar in size for the B_y negative case. These observations are consistent with the empirical plasma convection patterns described by Heppner and Maynard (10). Neutral horizontal winds in the F-region obtained from the VSH model indicates a good correspondence with observations acquired at Søndre Strømfjord during periods in which this station is within the polar cap. The greatest discrepancy between modelled and measured winds occurs during the cusp transit over Søndre Strømfjord.

ACKNOWLEDGEMENTS

Dr. Johnson's efforts were funded under NSF Grant ATM-9096134 and by the Air Force Office of Space Research under contract F49620-87-K-0007. This research was also supported by NSF Grant ATM-8822530 and by the Air Force through grant F19628-89-K-0047.

REFERENCES

1. F. G. McCormac and R. W. Smith, The influence of the interplanetary magnetic field Y component on ion and neutral motions in the polar thermosphere, *Geophys. Res. Lett.* 11, 935 (1984).
2. F. G. McCormac, T. L. Killeen, E. Gombosi, P. B. Hays and N. W. Spencer, Configuration of the high-latitude thermosphere neutral circulation for IMF B_y negative and positive, *Geophys. Res. Lett.* 12, 155 (1985).
3. J. W. Meriwether, Jr. and P. Shih, On the nighttime signatures of thermospheric winds observed at Sondrestrom, Greenland, as correlated with interplanetary magnetic field parameters, *Ann. Geophys.*, 5A, 1987, p. 329.
4. J. W. Meriwether, Jr., T. L. Killeen, F. G. McCormac, A. G. Burns and R. G. Roble, Thermospheric winds in the geomagnetic polar cap for solar minimum conditions, *J. Geophys. Res.* 7478 (1988).
5. R. J. Sica, G. Hernandez, B. A. Emery, R. G. Roble, R. W. Smith and M. H. Rees, The control of auroral zone dynamics and thermodynamics by the interplanetary magnetic field dawn-dusk (Y) component, *J. Geophys. Res.* 94, 11921 (1989).
6. O. de la Beaujardière and V. B. Wickwar, IMF control of plasma drift, ion temperature, and neutral wind, in *Proceedings of the Third Finnish-American Auroral Workshop*, edited by E. Turunen and E. Kataja, 1, 1985.
7. J. P. Thayer, T. L. Killeen, F. G. McCormac, C. R. Tschan, J.-J. Ponthieu and N. W. Spencer, Thermospheric neutral wind signatures dependent on the east-west component of the interplanetary magnetic field for northern and southern hemispheres as measured from Dynamics Explorer-2, *Ann Geophys.* 5A, 1987, p. 363.
8. D. Rees, T. J. Fuller-Rowell, R. Gordon, M. F. Smith, N. C. Maynard, J. P. Heppner, N. W. Spencer, L. Wharton, P. B. Hays and T. L. Killeen, A theoretical and empirical study of the response of the high latitude thermosphere to the sense of the "Y" component of the interplanetary magnetic field, *Planet. Space Sci.* 34, 1 (1986).
9. T. L. Killeen, R. G. Roble and N. W. Spencer, A computer model of global thermospheric winds and temperatures, *Adv. Space Res.* 7, 207 (1987).
10. J. P. Heppner and N. C. Maynard, Empirical high-latitude electric field models, *J. Geophys. Res.* 92, 4467 (1987).

APPENDIX B

F-Region Neutral Winds at Søndre Strømfjord: IMF By and Bz Dependences from Fabry-Perot and Incoherent Scatter Measurements

R. J. NICIEJEWSKI, T. L. KILLEEN, and R. M. JOHNSON (All at: Space Physics Research Laboratory, Department of Atmospheric and Oceanic Science, The University of Michigan, Ann Arbor, MI 48109-2143 USA)

Measurements of F-region neutral winds at Søndre Strømfjord have been routinely made by a Fabry-Perot interferometer since early 1983. Incoherent scatter experiments in the field aligned direction have coincided with some of the optical observations. In particular, neutral F region winds have been extracted from 76 radar experiments totalling 2200 hours observing time between April 1983 and July 1988. The incoherent scatter data analysis has shown that the IMF By component has a significant effect on the meridional wind: for $B_y < 0$, equatorward winds are enhanced for the nightside as compared to $B_y > 0$ conditions. The current study supplements the previous analysis by extending the database to include neutral winds measured by the Fabry-Perot interferometer. The dependence on the neutral meridional wind of the various permutations of IMF By and Bz positive and negative will be presented and discussed for the total database.

An Investigation of a Polar Cap Arc Sequence Using Ground-Based Measurements at Thule, Greenland

E. S. TRUDELL, T. L. KILLEEN, and R. J. NICIEJEWSKI, (All at: Space Physics Research Laboratory, Department of Atmospheric and Oceanic Science, The University of Michigan, Ann Arbor, MI 48109-2143 USA)

SU. BASU, (Institute for Space Research, Boston College, Newton, MA 02159)

B. W. REINISCH, (University of Lowell Center for Atmospheric Research, 450 Aiken St., Lowell, MA 01854)

An investigation of a series of polar cap arcs will be presented. Data obtained on 12 December 1988 during a High Latitude Plasma Structure (HLPS) campaign will be used to discuss the structure and dynamic behavior of the upper atmosphere during this occurrence. A series of OI (6300 Å) and OI (5577 Å) all-sky images and Fabry-Perot interferometer measurements were acquired at the University of Michigan airglow facility in Thule, Greenland ($\lambda=86^\circ$) on December 12, 1988 from 0851 UT to 1120 UT. The all-sky images depict intense sun-aligned arcs later followed by several diffuse, horseshoe-shaped arcs. Simultaneous FPI data obtained for both OI emissions show elevated temperatures, and initially, strong anti-sunward winds. Additional data has been obtained through digisonde measurements in the form of electron densities and ion drifts, and irregularity drift measurements using the spaced receiver scintillation technique. These data will be used along with the optical signature of the arcs to describe the morphology and dynamics at altitudes of 110 kilometers using the OI (5577 Å) emission and 220 kilometers using the OI (6300 Å) emission.

Ground Based OI (6300 Å) Fabry Perot Interferometer Observations from Thule and Søndre Strømfjord, Greenland: Systematics in the F Region Neutral Winds Observed Concurrently by Both Instruments

R. J. NICIEJEWSKI, J. P. THAYER, and T. L. KILLEEN (All at: Space Physics Research Laboratory, Department of Atmospheric and Oceanic Science, The University of Michigan, Ann Arbor, MI 48109-2143 USA)

Measurements of polar upper atmosphere OI (6300 Å) emissions by Fabry Perot interferometers at both Thule and Søndre Strømfjord, Greenland, have been acquired since 1986. Previously, studies of the systematics of F region neutral winds have been performed using only a single station [eg. Niciejewski et al, EOS, 1989]. The two stations are separated by ~900 km, and thus during clear sky conditions, both Fabry Perot interferometers can simultaneously observe a large portion of the polar cap F region. In this presentation, we will discuss results from two modes of operation: 1) concurrent observations of the same volume from both stations obtained during the 1987/88 observing season, and 2) independent meridional and zonal neutral wind observations obtained at the same time from both stations. The latter will be compared with VSH model predictions of the neutral winds for a case of low geomagnetic activity.

Ground-based observations of ion/neutral coupling at Thule and Qânâq, Greenland: IMF B_z dependence

J. P. THAYER, R. J. NICIEJEWSKI, and T. L. KILLEEN, (All at: Space Physics Research Laboratory, Department of Atmospheric and Oceanic Science, The University of Michigan, Ann Arbor, MI 48109-2143 USA)

J. BUCHAU, (Geophysics Lab, Hanscom AFB, Bedford, MA 01731-5000)

B. W. REINISCH, and G. CROWLEY (Both at: University of Lowell Center for Atmospheric Research, 450 Aiken St., Lowell, MA 01854)

During December, 1988, twenty-four hours of darkness and clear sky conditions permitted continuous observations of the OI (6300Å) airglow by a Fabry-Perot interferometer located at Thule, Greenland. Thus, a long term continuous record of the F-region neutral winds was obtained for that month. During this same time period, a digital ionosonde located at Qânâq, Greenland (110 km due north of Thule) was in operation measuring electron density profiles and F-region ion drifts. Using these diagnostics, a one to one correspondence between the F-region neutral wind and the ion drift measurements may be established. This allows for the investigation of ion/neutral coupling from the ground-based observations at a temporal resolution of about 15 minutes. From the 16th to the 24th of December, IMF data from the IMP 8 satellite were available and indicated intervals of B_z directed northward IMF conditions during this period. Signatures of sunward directed neutral winds and ion drifts were observed coincident with northward IMF. The response of the neutral winds to sunward ion drifts under B_z northward conditions is investigated.

Niciejewski, R. J., T. L. Killeen, R. M. Johnson, and J. Thayer, The behaviour of the high-latitude F-region neutral thermosphere in relation to IMF parameters

Ground based incoherent scatter radar and Fabry Perot interferometer studies in the northern high latitudes during the period 1983 to 1989 have shown that the F-region neutral wind field pattern depends upon the sign of the IMF parameters. For example, the cell structure of the northern hemisphere high latitude neutral wind field during periods of low geomagnetic activity depends to a large degree upon the sign of the IMF B_y parameter. Long term monitoring of the F-region thermosphere by FPI in Thule, Greenland, and by both FPI and ISR in Søndre Strømfjord, Greenland, have made it possible to produce maps of average meridional and zonal wind fields for various IMF configurations for northern high latitudes. Comparison of observations with theoretical wind field modelling, such as the Vector Spherical Harmonic model, indicates that most observed features are within the context of the models.

Fabry Perot interferometer observations of neutral winds in the polar cap during northward IMF

R. J. NICIEJEWSKI, T. L. KILLEEN, and Y. WON (All at: Space Physics Research Laboratory, Department of Atmospheric and Oceanic Science, The University of Michigan, Ann Arbor, MI 48109-2143 USA)

Remote observations of F-region neutral winds have been performed by the University of Michigan at Thule Air Base (lat: 76.5 °N, long: 69.0 °W) and Søndre Strømfjord (lat: 67.0 °N, long: 50.9 °W), Greenland, since early 1983. The former site is located well within the polar cap, while the latter is situated beneath the auroral oval during dawn and dusk, and within the polar cap at night. Nearly a complete solar cycle of data are currently available. The sign of the B_z component of the IMF plays an important role in the dynamics of the polar cap ionosphere, and through ion drag forcing, the polar cap thermosphere. Observations indicate that the anti-sunward horizontal neutral wind component at F region altitudes is much reduced during northward IMF conditions. Examples of these measurements will be shown and discussed relative to standard diurnally reproducible Vector Spherical Harmonic (VSH) model representations of the neutral wind field for 250 km altitude. Averaged horizontal neutral winds for both signs of B_z for both sites will also be displayed and discussed.

GROUND-BASED OPTICAL MEASUREMENTS FROM WITHIN THE
GEOMAGNETIC POLAR CAP AT THULE, GREENLAND ($\Lambda=86^\circ$)

T. L. Killeen*, R. J. Niecejewski, Y. Won,
and G. S. N. Murty
Space Physics Research Laboratory
Department of Atmospheric, Oceanic, and Space Sciences
The University of Michigan
Ann Arbor, Michigan 48109-2143

Observations of the dynamics and thermodynamics of the polar cap thermosphere have been obtained routinely since the winter of 1984 with an automated optical observatory located at Thule, Greenland ($\Lambda=86^\circ$). The instrumentation at the observatory includes a Fabry-Perot interferometer (FPI), a half-meter Ebert-Fastie spectrophotometer (EFS), and a digital all-sky camera (ASC) system. The FPI has a 10 cm etalon coated for operation between 5577-Å and 7320-Å and an image plane detector similar to that flown on the Dynamics Explorer spacecraft. The FPI and EFS instruments are controlled automatically throughout each 8-month winter observing season (September - April) with an LSI 11/23 computer system and CAMAC interface cards. The ACS is operated on a campaign basis. The thermospheric neutral winds and temperatures measured with the FPI in the years 1985-1991 show strong dependencies on the solar cycle, local time, geomagnetic activity level and interplanetary magnetic field orientation. The EFS has been used to observe various nightglow emissions including NI (5200-Å), OI(5577-Å), OI(6300-Å), Balmer H α (6563-Å), OII(7320-30-Å), and the OH (8-3) vibrational band. The ACS has been used in conjunction with the FPI to correlate sun-aligned polar cap arcs and thermospheric dynamics. This paper will describe the current status and plans for the automated optical observatory at Thule and will discuss several of the more significant scientific findings made over the past several years.

OBSERVATIONS OF NEUTRAL WINDS IN THE POLAR CAP DURING NORTHWARD IMF

by

R. J. Niciejewski, T. L. Killeen, and Y. Won
Space Physics Research Laboratory,
The University of Michigan
Ann Arbor, MI, USA 48109

Long term remote observations of neutral winds at F-region altitudes have been performed at Thule Air Base (lat: 76.5° N, long: 69.0 W), Greenland, and Søndre Strømfjord (lat: 67.0 N, long: 50.9 W), Greenland, since 1983. The former site is very close to the geomagnetic pole, while the latter site is within the polar cap for several hours each night on either side of geomagnetic midnight. The data base that currently exists corresponds to nearly one full solar cycle. This paper will present the following: one hour averages of thermospheric neutral winds for northward IMF conditions obtained by both instruments binned according to the sign of B_y ; individual data sets from Thule showing the dependence of the neutral wind on the sign of B_z ; and deviations of the averaged northward IMF measurements from standard diurnally reproducible Vector Spherical Harmonic (VSH) representations of the polar cap neutral wind field for 250 km altitude. Thermospheric wind measurements at Thule Air Base during northward IMF very often show a dramatic reduction in the anti-sunward horizontal wind component. Examples of these measurements will be shown.

Dr. Richard J. Niciejewski,
Assistant Research Scientist
Space Physics Research Laboratory
The University of Michigan
Ann Arbor, MI, USA 48109

Preferred symposium: GAM 2.11/3.10
Presentation preference: poster

The Northern, High Latitude Thermosphere: Neutral Temperatures and Winds During the 1991/92 Optical Observing Season

R. J. NICIEJEWSKI, T. L. KILLEEN, Y. WON, and M. TURNBULL (All at: Space Physics Research Laboratory, Department of Atmospheric and Oceanic Science, The University of Michigan, Ann Arbor, MI 48109-2143 USA)

Fabry-Perot interferometer observations of the thermosphere are currently being performed from several locations in the northern hemisphere by an aeronomy group at the University of Michigan in support of several efforts: the CEDAR program, the UARS ground support program, and the SPIRIT II ground support effort. This current observing season, late August '91 to late April '92, coincides with an apparent increase in solar activity, and the subsequent heating of the terrestrial thermosphere and increase in geomagnetic activity. Neutral winds (both vertical and horizontal) and neutral temperatures are routinely obtained from these sites, which encompass a wide range of latitudes and local times. In this presentation, the current set of geophysical measurements will be compared with previous measurements from the decline phase of the previous solar cycle (1983 onwards), and with the current state-of-the-art VSH model. In addition, the utility of combining multi-station observations on single "weather maps" will be presented for various events, including the 2/8 - 2/9, 1992, geomagnetic storm ($A_p = 65$, $K_p \leq 7$).

Seasonal and Diurnal Variability in the Northern High Latitude Thermosphere: Neutral Temperatures and Horizontal Winds

R. J. NICIEJEWSKI, T. L. KILLEEN, and Y. WON (All at: Space Physics Research Laboratory, Department of Atmospheric and Oceanic Science, The University of Michigan, Ann Arbor, MI 48109-2143 USA)

Ground based measurements of the neutral wind and neutral temperature in the thermosphere have been made for both solar minimum and solar maximum conditions from two stations in the high northern latitudes: Thule Air Base and Søndre Strømfjord, Greenland. For this study, which is a part of the Coordinated Analysis of the Thermosphere effort (CAT), the data sets have been screened to include only periods of low geomagnetic activity ($K_p < 3$) and have been hourly binned for two month intervals centered on the autumnal equinox, the winter solstice, and the vernal equinox. Both the averaged winds and the averaged temperatures show interesting seasonal and diurnal variations. The thermosphere above Søndre Strømfjord is cooler during the winter season compared to the equinoxes, the meridional winds are less in magnitude during the winter, and the zonal winds are similar for all seasons. Variability in the seasonal behavior above Thule Air Base is not as marked in contrast to that above Søndre Strømfjord. However, the diurnal variability in the thermosphere above Thule Air Base is more pronounced than that above Søndre Strømfjord: both the zonal and the meridional winds exhibit diurnal variations nearly double for the northern location compared to the southern site. The binned data will be presented with least square fits describing both the diurnal and the semi-diurnal components, as well as compared to recent numerical models, and the underlying driving processes will be discussed.

Fabry-Perot Interferometric Measurements of Mesopause and Lower Thermospheric Structure

T. L. Killeen and R. J. Niciejewski (Space Physics Research Laboratory, The University of Michigan, Ann Arbor, MI 48109; 313-747-3430)

Fabry-Perot interferometric techniques have been applied in recent years to investigate the thermal and dynamical structure of the mesopause and lower thermosphere from the ground as well as from space. This paper provides a review of the new instrumental approaches and geophysical results gained using the Fabry-Perot technique. Comparisons with numerical and empirical models will be shown. Emphasis will be placed on the results obtained with the University of Michigan's chain of optical observatories.

1. Chapman Conference on the Upper Mesosphere and Lower Thermosphere

2. Invited Oral

3. Timothy L. Killeen
Space Physics Research Lab
The University of Michigan
2455 Hayward
Ann Arbor, MI 48109

313-747-3435

Observations of high-latitude thermospheric neutral winds over a half solar cycle from Thule Air Base and Søndre Strømfjord, Greenland

Y. WŦN, T. L. KILLEEN, and R. J. NICIEJEWSKI (All at: Space Physics Research Laboratory, Department of Atmospheric and Oceanic Science, The University of Michigan, Ann Arbor, MI 48109-2143 USA)

Ground-based Fabry-Perot interferometers (FPIs) at Thule Air Base and Søndrestrøm, Greenland have been used to determine the dynamical and thermodynamical properties of the thermosphere by measuring emission line profiles from the O(¹D) and O(¹S) nightglow at high spectral resolution. Data has been obtained routinely since the winter of 1984 with the FPIs at two automated optical observatories located at Thule Air Base and Søndre Strømfjord, Greenland. The multi-year data base has been analyzed to determine the average dependence of the high-latitude thermospheric circulation pattern as a function of solar cycle, K_p, IMF orientation, and solar F10.7. The observed winds, obtained over a period corresponding to half a solar cycle (1985 - 1991), have been compared with the predictions of the VSH and HWM models of thermosphere dynamics. This period encompasses both solar minimum and solar maximum conditions. We present the averaged data sets from the combined Thule and Søndrestrøm observations and discuss them in the context of the model predictions.

Studies of High-Latitude Lower Thermospheric Dynamics Based on Measurements and Modelling of Lower Thermospheric Coupling Study Experiments

R. M. Johnson, Y. Won, R. Niecejewski, and T. L. Killeen (Space Physics Research Laboratory, The University of Michigan, Ann Arbor, MI 48109; 313-747-3430)
T. S. Viridi and P. J. S. Williams (both at Physics Dept., University College Wales, UK)
A. H. Manson and C. E. Meek (both at ISAS, University of Saskatchewan, Canada)
R. A. Vincent (University of Adelaide, Australia)
G. H. Fraser (University of Canterbury, New Zealand)
J. Forbes (Dept. of Electrical, Computer, and Systems Engineering, Boston University, MA)
C. Fesen (Thayer School of Engineering, Dartmouth College, Hanover, NH)
R. Roble (High Altitude Observatory, NCAR, Boulder, CO)

Observations obtained by high-latitude radars and optical instruments during Lower Thermospheric Coupling Study experiments, in conjunction with modelling studies, allow us to make significant advances in our understanding of the structure and dynamics of the lower thermosphere. Seasonal variations in high-latitude lower thermospheric mean winds and temperatures and diurnal and semidiurnal "tidal" components are apparent in observations. During periods of intense geomagnetic activity, evidence for accelerated neutral flows in the lower thermosphere can be found. Comparison of observational results with TIGCM simulations of LTCS experiments generally shows some agreement with the features seen in the data, although the magnitude of the features are generally smaller and the timing slightly different in the model results. Semidiurnal tidal amplitudes determined from high-latitude LTCS measurements are generally larger than those calculated using tidal models, and there are significant variations in observed and modelled phase profiles.

1. Chapman Conference on the Upper Mesosphere and Lower Thermosphere

2. Invited Oral

3. Roberta M. Johnson
Space Physics Research Lab
The University of Michigan
2455 Hayward
Ann Arbor, MI 48109

313-747-3430

Seasonal variation of winds in the high latitude lower thermosphere/upper mesosphere at Thule Air Base and Søndre Strømfjord, Greenland.

Y. Won, T L Killeen, R M Johnson and R J Niciejewski
(Space Physics Research Laboratory, Department of Atmospheric, Oceanic, and Space Sciences, The University of Michigan, Ann Arbor, MI 48109-2143)

Ground-based Fabry-Perot interferometers (FPI) have been used to determine dynamical properties of the lower thermosphere/upper mesosphere by measuring emission line profiles from the O(¹S) nightglow at high spectral resolution. The resulting winds are normally referred to the altitude of the peak of the O(¹S) emission layer, near 97 km. Data has been obtained since the winter of 1987 at two optical observatories located at Thule Air Base and Søndre Strømfjord, Greenland. In our analysis, data have been removed during periods of cloud cover and high signal intensity to eliminate auroral contaminations. Average neutral winds are calculated and spectral analysis is carried out to examine the major tidal wind components. The seasonal variations of these wind components will be discussed and compared to model predictions.

1. 1992 AGU Chapman conference on the upper mesosphere and lower thermosphere
2. (b) poster presentation
3. (a) Youngin Won
The University of Michigan
Space Physics Research Lab.
2455 Hayward
Ann Arbor, MI 48109-2143

(b) 313-747-3450

Tides in the lower thermosphere and upper mesosphere from optical and radar measurements and model results

Y. WON, R. M. JOHNSON, T. L. KILLEEN, and R. J. NICIEJEWSKI (All at: Space Physics Research Laboratory, Department of Atmospheric and Oceanic Science, The University of Michigan, Ann Arbor, MI 48109-2143 USA)
J. M. FORBES (High Altitude Observatory, National Center for Atmospheric Research, Boulder, CO, 80307)

Measurements of winds in the lower thermosphere and upper mesosphere region were obtained from various ground-based Fabry-Perot interferometers and incoherent scatter radar observatories. Tidal information was then extracted by performing harmonic analysis on these data. The day-to-day variation of these tidal fields are discussed in this presentation, in addition to our description of the seasonal characteristics. The amplitudes and phases of the seasonally averaged data are utilized to obtain an empirical description of the semidiurnal tidal fields by using a set of numerically generated "Hough Mode Extension" (HME) functions for u , v , and δt corresponding to the (2,2), (2,3), (2,4), and (2,5) semidiurnal tidal modes. The results will be compared with tidal fields from the Forbes and Vial (1989) numerical tidal model.

Thermospheric Neutral Wind Climatology in the Northern High Latitudes

R. J. NICIEJEWSKI (Space Physics Research Laboratory, Department of Atmospheric and Oceanic Science, The University of Michigan, Ann Arbor, MI 48109-2143 USA)
J. P. THAYER (SRI International, Geoscience and Engineering Center, Menlo Park, CA 94025)
A. L. Aruliah (University College London, England)

As part of the Coordinated Analysis of the Thermosphere (CAT), a high-latitude working group was formed to analyze and interpret the diurnal/seasonal/solar cycle variations in the observed thermospheric neutral wind during geomagnetically quiet conditions. The high-latitude sites which have participated in the study include Thule, Greenland (76.5N, -68.4E), Sondrestrom, Greenland (67.0N, -50.9E), and Kiruna, Sweden (67.8N, 20.4E). The Thule, Sondrestrom, and Kiruna sites provide full vector winds from Fabry-Perot interferometer (FPI) measurements of the thermospheric 6300Å emission while thermospheric neutral winds in the magnetic meridian are derived from the incoherent-scatter radar (ISR) measurements at Sondrestrom. A large database of thermospheric neutral winds has been compiled covering an entire solar cycle (1981 - 1991). The FPI data are limited to nighttime observations and therefore exclude the summer season as well as some daytime hours throughout the year. Comparisons of these data sets with the NCAR TIGCM simulation and the HWM90 empirical model will be presented. A harmonic analysis was applied to the averaged ISR meridional winds to demonstrate the daily variability and the seasonal dependence of the fitted harmonics. Care must be taken in interpreting the harmonic analysis as tidal in nature as the forcing by the two-cell ion convection will introduce a semidiurnal influence on the observations.

APPENDIX C

**NEUTRAL WIND VORTICES IN THE HIGH-LATITUDE
THERMOSPHERE**

by

Jeffrey Paul Thayer

**A dissertation submitted in partial fulfillment
of the requirements for the degree of
Doctor of Philosophy
(Atmospheric and Space Sciences)
in The University of Michigan
1990**

Doctoral Committee:

**Associate Professor, Timothy L. Killeen, Chairman
Professor, John P. Boyd
Assistant Professor, Mary L. Brake
Research Scientist, William E. Sharp**

**STUDIES OF THERMOSPHERIC NEUTRAL WINDS UTILIZING
GROUND-BASED OPTICAL AND RADAR MEASUREMENTS**

by

Youngin Won

**A dissertation submitted in partial fulfillment
of the requirements for the degree of
Doctor of Philosophy
(Atmospheric and Space Sciences)
in The University of Michigan
1994**

Doctoral Committee:

**Professor Timothy Killeen, Co-Chair
Associate Research Scientist Roberta Johnson, Co-Chair
Professor Anthony England
Professor Andrew Nagy
Assistant Research Scientist Richard Niciejewski**